

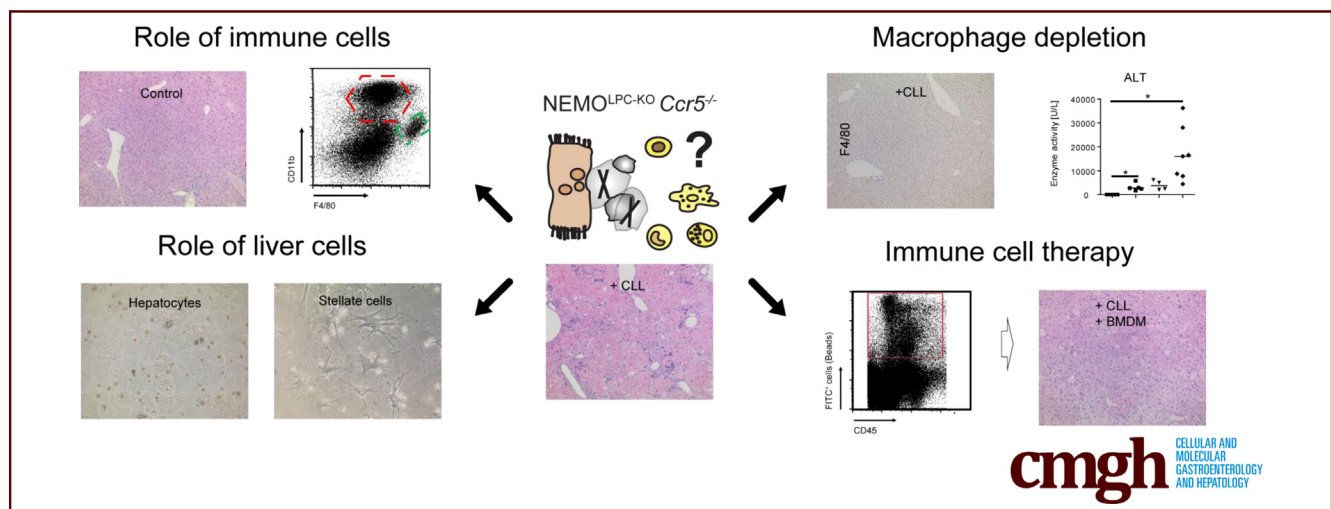
ORIGINAL RESEARCH

Roles of CCR2 and CCR5 for Hepatic Macrophage Polarization in Mice With Liver Parenchymal Cell-Specific NEMO Deletion



Matthias Bartneck,^{1,*} Christiane Koppe,^{1,*} Viktor Fech,¹ Klaudia T. Warzecha,¹ Marlene Kohlhepp,^{1,2} Sebastian Huss,³ Ralf Weiskirchen,⁴ Christian Trautwein,¹ Tom Luedde,^{1,5,§} and Frank Tacke^{1,2,§}

¹Department of Medicine III, RWTH Aachen University, Aachen, Germany; ²Department of Hepatology and Gastroenterology, Charité University Medicine Berlin, Berlin, Germany; ³Gerhard Domagk Institute of Pathology, University Hospital Münster, Münster, Germany; ⁴Institute of Molecular Pathobiochemistry, Experimental Gene Therapy and Clinical Chemistry, RWTH University Hospital Aachen, Aachen, Germany; and ⁵Department of Gastroenterology, Hepatology and Infectious Diseases, University Hospital Düsseldorf, Medical Faculty of Heinrich Heine University Düsseldorf, Düsseldorf, Germany



SYNOPSIS

Macrophages critically regulate liver inflammation. Using a genetically determined hepatitis mouse model we found that CCR2 controls monocyte and macrophage recruitment to injured livers, while CCR5-dependent functions of liver macrophages limit hepatic injury, thereby reducing steatosis and hepatocarcinogenesis.

BACKGROUND & AIMS: Macrophages are key regulators of inflammation and cancer promotion in the liver, and their recruitment and activation is linked to chemokine receptor signaling. However, the exact roles of the chemokine receptors CCR2 and CCR5 for macrophage functions in the liver is obscure.

METHODS: To study CCR2 and CCR5 in inflammatory liver injury, we used mice with a hepatocyte-specific knock-out of the nuclear factor κ B (NF- κ B) essential modulator (NEMO), termed NEMO^{LPC-KO} mice, and generated NEMO^{LPC-KO}Ccr2^{-/-} and NEMO^{LPC-KO}Ccr5^{-/-} mice. NEMO^{LPC-KO} mice develop hepatitis and fibrosis after two and liver tumors after six months.

RESULTS: We found that both CCR2 and CCR5 deficiency led to reduced fibrosis, while CCR5 deficiency increased steatosis and tumor burden in NEMO^{LPC-KO} mice. CCR2 was required for recruitment of hepatic macrophages, whereas CCR5 promoted stellate cell activation. The reduction of monocytes and macrophages by either anti-Gr1 antibody or clodronate-loaded liposomes (CLL), but not of CD8⁺ T cells or NK cells, significantly aggravated liver injury in NEMO^{LPC-KO} mice and was further increased in NEMO^{LPC-KO}Ccr5^{-/-} mice. CLL-induced liver injury was dampened by the adoptive transfer of *ex vivo* generated macrophages, whereas the adoptive transfer of control CD115⁺ immature monocytes or B cells did not reduce liver injury.

CONCLUSIONS: Although CCR2 and CCR5 principally promote liver fibrosis, they exert differential functions on hepatic macrophages during liver disease progression in NEMO^{LPC-KO} mice. While CCR2 controls the recruitment of monocytes to injured livers, CCR5-dependent functions of liver macrophages limit hepatic injury, thereby reducing steatosis and hepatocarcinogenesis. (*Cell Mol Gastroenterol Hepatol* 2021;11:327–347; <https://doi.org/10.1016/j.jcmgh.2020.08.012>)

Keywords: Hepatitis; Cell Therapy; Macrophages; Liver Cancer.

Deletion of the nuclear factor kappa B essential modulator (NEMO), also known as nuclear factor kappa B inhibitor of kinase subunit gamma, in liver parenchymal cells (LPCs) induces spontaneous hepatitis and hepatocyte apoptosis. The inflammatory process leads to a regenerative response of the liver resulting in a sequence of steatohepatitis, fibrosis, and, ultimately, liver cancer.¹ This sequence of disease progression represents a valuable murine model for inflammatory hepatocarcinogenesis initiated by a specialized genetic deficiency, as it reflects hallmarks of liver disease progression in humans.²

Macrophages are among the most numerous immune cell types in the liver and are critically involved in regulating inflammation and cancer. They exhibit a unique plasticity, with classically activated (M1) macrophages or alternatively activated (M2) macrophages representing 2 extreme facets of a broad spectrum.³ Macrophages in injured livers mainly originate from monocytes that translocate into the liver upon injury and express F4/80, CD11b, and the Ly6C antigen on their surface in mice. The recruitment of these monocyte-derived macrophages (MoMFs) to injured livers is mediated by the CC-chemokine receptor type 2 (CCR2), which is a pharmacological target in the treatment of liver fibrosis and nonalcoholic steatohepatitis (NASH).⁴ Kupffer cells (KCs) are resident liver macrophages, which express high levels of F4/80 and CLEC4F but low levels of Ly6C and CD11b in mice.⁵ Macrophages accompany tumor progression at different stages, with a role in early initiation and tissue invasion, as well as in facilitating immunosuppression at later stages.⁶

In general, the migration of subgroups of immune cells into the liver is mediated by chemokine receptors. We have recently shown that blocking CC motif chemokine 2 (CCL2), the prime ligand for CCR2, in a mouse model for liver cancer impacts angiogenic macrophage populations in the tumor environment.⁷ CCR2 is expressed by Ly6C⁺ (Gr1⁺) monocytes, which infiltrate the liver upon injury in mice.⁸ Thus, deficiency in CCR2 is associated with reduced infiltration of the liver with monocyte macrophages and ameliorated liver injury.⁸ The CC-chemokine receptor 5 (CCR5) and its ligands CCL3–CCL5 have been linked to human and murine liver injury progression and represent a potential therapeutic target for patients with chronic liver disease.⁹ Importantly, the CCR2/CCR5 inhibitor cenicriviroc is currently under phase 3 clinical investigation in patients with NASH and advanced fibrosis,¹⁰ who represent a high-risk group for liver cancer. Presumably, CCR2/CCR5 inhibitors target not only inflammatory cells, but also CCR5-expressing hepatic stellate cells (HSCs), the key cell type for liver fibrosis that can produce extracellular matrix proteins. The activation and transdifferentiation of HSCs into myofibroblasts that are contractile and produce extracellular matrix is driven by autocrine- and paracrine-acting soluble mediators such as cytokines and chemokines.¹¹ HSCs express CCR5 but are also affected by signals from other cells like macrophages. We have recently demonstrated that CCL2 inhibition also has an indirect inhibitory effect on HSCs collagen I and IV expression by reducing fibrogenic and angiogenic macrophages in the liver.⁷

In this study, we aimed at understanding the roles of CCR2 and CCR5 in the pathogenesis of chronic liver disease

from injury to inflammation, fibrosis, and cancer by using wild-type (WT) and knockout (KO) (NEMO^{LPC-KO}, NEMO^{LPC-KO} Ccr2^{-/-}, and NEMO^{LPC-KO} Ccr5^{-/-}) mice. The NEMO^{LPC-KO} mice represent a unique mouse model to study the progression of chronic liver diseases from hepatitis, steatosis, and fibrosis (at an early age of 8 weeks) as well as primary liver cancer (at 26 weeks of age). In order to determine the role of different immune cells for the spontaneous liver injury in the different mouse strains, we used various monoclonal antibodies to deplete immune cell subsets and clodronate-loaded liposomes (CLLs) to diminish hepatic macrophages (particularly MoMF). We identified an important, CCR5-dependent regulatory function of hepatic macrophages in preventing excessive liver injury, highlighting the critical function of macrophages for restoring tissue homeostasis in the liver.

Results


CCR2 and CCR5 Deficiency Differentially Affects Spontaneous Liver Injury, Inflammation, Fibrosis, and Cancer in NEMO^{LPC-KO} Mice

The chemokine receptors CCR2 and CCR5 are currently targeted in clinical trials on NASH. The A Phase III, Multi-center, Randomized, Double-Blind, Placebo-Controlled Study to Evaluate the Efficacy and Safety of Cenicriviroc for the Treatment of Liver Fibrosis in Adult Subjects With Nonalcoholic Steatohepatitis study (NCT03028740) investigates cenicriviroc, an oral, small molecule-based dual CCR2/CCR5 antagonist with nanomolar potency against both receptors, for the treatment of liver fibrosis in adults with NASH.¹² In rodent studies, cenicriviroc significantly ameliorated steatohepatitis and fibrosis,¹³ presumably by reducing the infiltration of Ly6C⁺ monocytes.⁴ In order to better understand differential effects of CCR2 and CCR5 on liver disease progression, we studied CCR2 and CCR5 deficiency separately on the background of the NEMO^{LPC-KO} model that age-dependently reflects human disease phases (steatosis, inflammation, fibrosis, cancer).

At 8 weeks of age, livers of NEMO^{WT}, NEMO^{LPC-KO}, NEMO^{LPC-KO} Ccr2^{-/-}, and NEMO^{LPC-KO} Ccr5^{-/-} mice were

*Authors share co-first authorship; §Authors share co-senior authorship.

Abbreviations used in this paper: ALT, alanine aminotransferase; BMDM, bone marrow-derived macrophages; CCL, CC motif chemokine; CCR, CC-chemokine receptor; CLL, clodronate-loaded liposome; HSC, hepatic stellate cell; IFN γ , interferon gamma; IL, interleukin; KC, Kupffer cell; KO, knockout; LPC, liver parenchymal cell; LPS, lipopolysaccharide; MoMF, monocyte-derived macrophage; mRNA, messenger RNA; NAFLD, nonalcoholic fatty liver disease; NASH, nonalcoholic steatohepatitis; NEMO, nuclear factor kappa B essential modulator; NK, natural killer; PDGF, platelet-derived growth factor; PPAR, Peroxisome proliferator-activated receptor; SREBP, sterol-regulatory element binding protein; TGF- β , transforming growth factor beta; TNF, tumor necrosis factor; WT, wild-type.

 Most current article

© 2020 The Authors. Published by Elsevier Inc. on behalf of the AGA Institute. This is an open access article under the CC BY-NC-ND license (<http://creativecommons.org/licenses/by-nc-nd/4.0/>).

2352-345X

<https://doi.org/10.1016/j.jcmgh.2020.08.012>

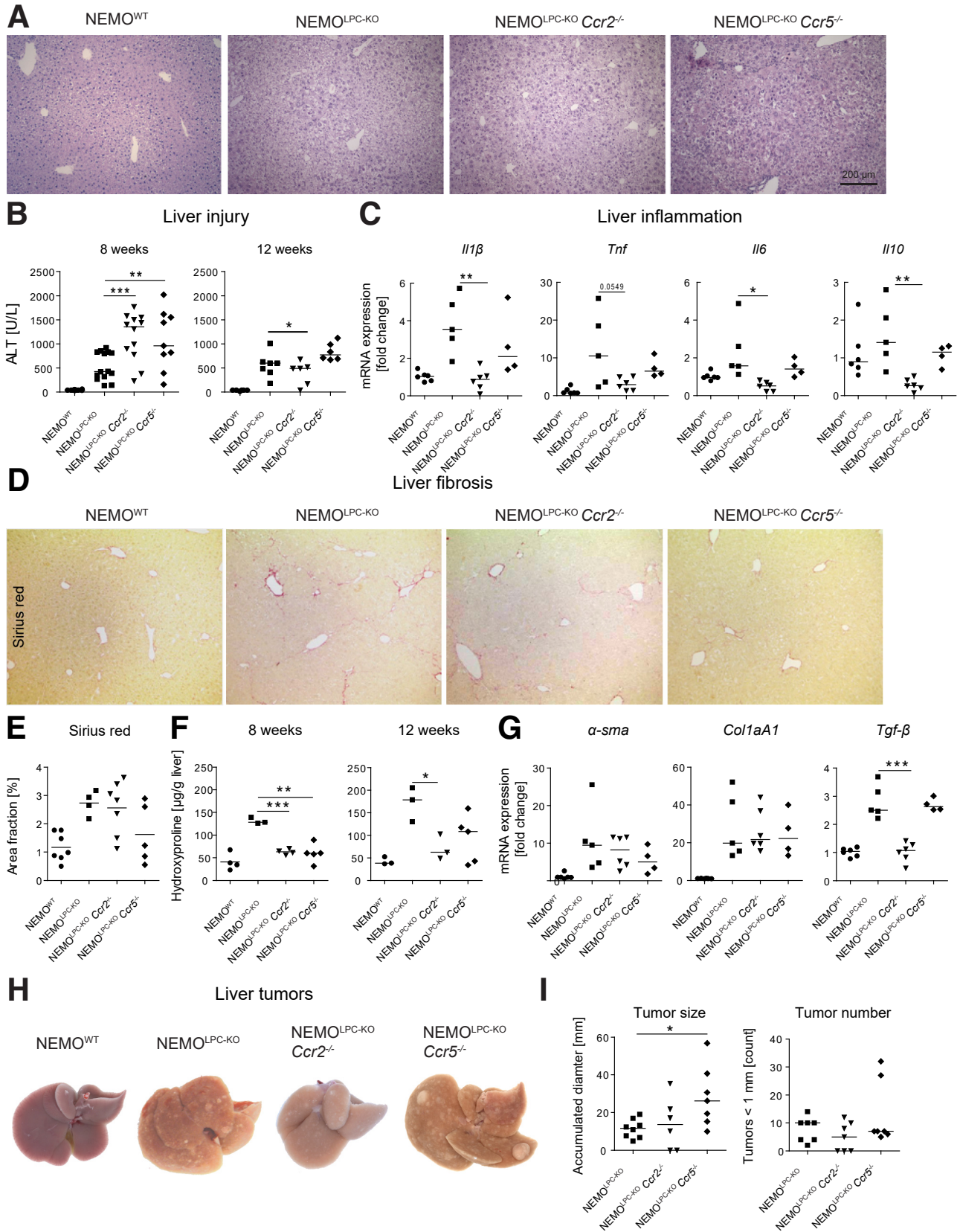


Figure 1. Effects of *Ccr2* or *Ccr5* deficiency on fibrosis, steatosis, and tumorigenesis in NEMO LPC-deficient mice. (A) Eight-week-old NEMO^{WT}, NEMO^{LPC-KO}, NEMO^{LPC-KO} *Ccr2*^{-/-}, and NEMO^{LPC-KO} *Ccr5*^{-/-} mice were analyzed for histology using hematoxylin and eosin staining and for (B) liver injury reflected by ALT after 8 and 12 weeks of age. (C) Hepatic inflammation assessed based on the expression of inflammatory mediators in whole liver. (D) Fibrosis quantification based on Sirius Red

analyzed using hematoxylin and eosin staining for liver histology. The livers of the NEMO^{LPC-KO}*Ccr5*^{-/-} mice exhibited a slightly more disturbed liver histology than did the NEMO^{LPC-KO} and NEMO^{LPC-KO}*Ccr2*^{-/-} mice (Figure 1A). Unexpectedly, liver injury reflected by alanine aminotransferase (ALT) was significantly increased in NEMO^{LPC-KO}*Ccr2*^{-/-} and NEMO^{LPC-KO}*Ccr5*^{-/-} mice compared with the NEMO^{LPC-KO} animals after 8 weeks, while after 12 weeks, NEMO^{LPC-KO}*Ccr2*^{-/-} mice showed a moderate reduction in ALT activity (Figure 1B). We further studied liver inflammation based on measuring the messenger RNA (mRNA) expression of the inflammatory cytokines interleukin 1 β (*Il1 β*), the tumor necrosis factor (*Tnf*), *Il6*, and the anti-inflammatory *Il10*. Interestingly, not only *Il1 β* and *Il6*, but also *Il10* were significantly downregulated in NEMO^{LPC-KO}*Ccr2*^{-/-} animals compared with the NEMO^{LPC-KO} mice. The mRNA expression of all cytokines of the NEMO^{LPC-KO}*Ccr5*^{-/-} mice were similar to that of the NEMO^{LPC-KO} background (Figure 1C). Thus, we have shown that CCR2 deficiency not only leads to a reduced expression of inflammatory, but also anti-inflammatory markers associated with wound healing.

In order to study consequences of the inflammatory setting on fibrogenesis, we performed Sirius Red staining of hepatic collagen (Figure 1D). We found that the fibrosis was slightly reduced in both NEMO^{LPC-KO}*Ccr2*^{-/-} and NEMO^{LPC-KO}*Ccr5*^{-/-} mice compared with the NEMO^{LPC-KO} mice, as outlined by quantifications of the Sirius Red area fraction (Figure 1E). Hepatic hydroxyproline, a major constituent of collagen, was quantified, which showed a more pronounced reduction by both chemokine receptor deficient compared with the NEMO^{LPC-KO} animals after 8 and 12 weeks (Figure 1F). We further measured fibrosis-associated mRNA alpha smooth muscle actin (*α -Sma*), collagen 1A1 (*Col1a1*), and transforming growth factor beta (*Tgf- β*). *Tgf- β* was significantly reduced by the NEMO^{LPC-KO}*Ccr2*^{-/-} mice, while *α -Sma* and *Col1a1* were only mildly reduced in the NEMO^{LPC-KO}*Ccr2*^{-/-} and NEMO^{LPC-KO}*Ccr5*^{-/-} animals (Figure 1G).

In this genetic model, NEMO^{LPC-KO} mice develop primary liver cancers after 6 months. We found a reduction in the tumor load of NEMO^{LPC-KO}*Ccr2*^{-/-}, and increased tumors in NEMO^{LPC-KO}*Ccr5*^{-/-} mice, as shown by representative macroscopic images (Figure 1H) and quantifications (Figure 1I). While the reduction in tumor load by CCR2 deficiency was expected, it was surprising that a lack of CCR5 would lead to increased tumor numbers.

CCR2 or CCR5 Deficiency Does Not Increase Susceptibility to Lipopolysaccharide Challenge in NEMO^{LPC-KO} Mice

We next tested whether the increased "spontaneous" liver injury in CCR2- or CCR5-deficient NEMO^{LPC-KO} mice,

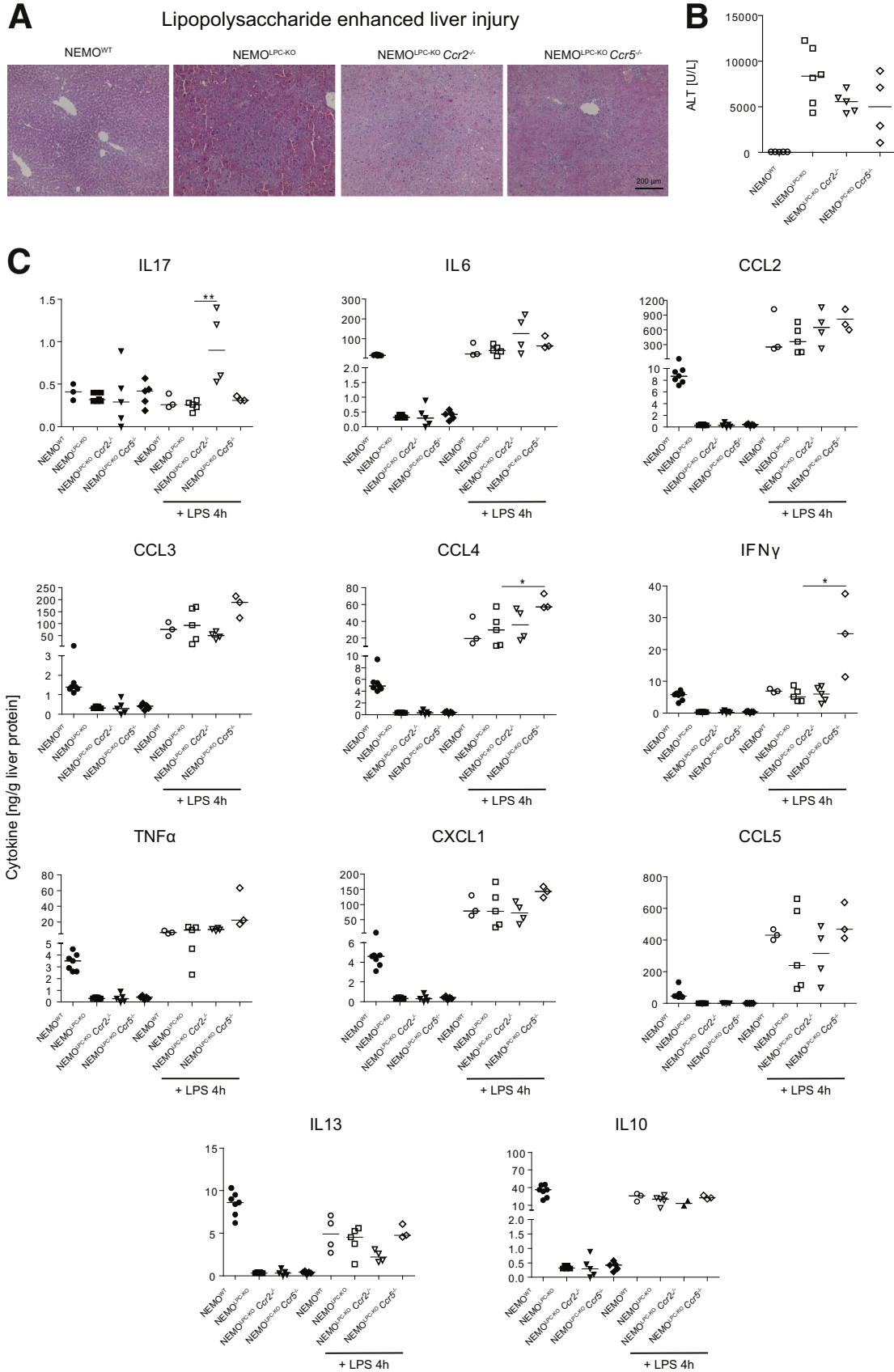
which was observed in the 8-week-old mice, would make these mice more vulnerable to an additional injury trigger. Therefore, we treated mice intraperitoneally with 0.42- μ g/kg lipopolysaccharide (LPS), which triggers tumor necrosis factor (TNF) release by KCs that subsequently induces massive apoptosis in livers of NEMO^{LPC-KO} mice (Figure 2A), as shown previously.¹ Surprisingly, CCR5 deficiency, and to a lesser extent CCR2 deficiency, ameliorated LPS-induced liver damage in NEMO^{LPC-KO} mice, as reflected by ALT (Figure 2B). Interestingly, the chemokine receptor deficiencies had an impact on LPS-triggered cytokine release. While in liver tissue of NEMO^{LPC-KO}*Ccr2*^{-/-} mice, IL17 and IL6 were elevated and IL13 and IL10 were reduced (Figure 2C). The NEMO^{LPC-KO}*Ccr5*^{-/-} mice showed significantly increased concentrations of the cytokines CCL4, interferon gamma (IFN γ), and TNF. Similar tendencies were noted also for CCL3, CCL5, and CXCL1. Interestingly, all 3 NEMO^{LPC-KO} mouse strains showed, if untreated, generally lower levels of most cytokines compared with the NEMO^{WT} mice, except for IL17 (Figure 2C). These data imply that important changes occur due to the chemokine receptor deficiencies, which might impact various processes in the body.

CCR5, But Not CCR2, Deficiency Increases Hepatic Triglyceride Accumulation in NEMO^{LPC-KO} Mice

Hepatic lipid accumulation is a hallmark of nonalcoholic fatty liver disease (NAFLD) in humans,¹⁴ which is also observed at young age in NEMO^{LPC-KO} mice.¹⁵ Oil red O, which stains hepatic lipids, demonstrated elevated fat deposition in the NEMO^{LPC-KO} mice, and a significant reduction of fat in the NEMO^{LPC-KO}*Ccr2*^{-/-} mice (Figure 3A and B). Free fatty acids in the serum, which were found to correlate with NAFLD in patients,¹⁶ were only mildly affected by the different mouse strains and were similar to the WT (Figure 3C). Importantly, hepatic triglyceride levels were markedly induced in 8-week-old NEMO^{LPC-KO}*Ccr5*^{-/-} mice (Figure 3D).

Hepatic steatosis is typically linked to specific changes in liver metabolism. We therefore studied the expression of selected mRNA associated with important metabolic functions. We found that glucose 6-phosphatase (*G6pase*), an enzyme that hydrolyzes glucose 6-phosphate and therefore increases the glucose serum levels, was not affected on the mRNA level. Interestingly, another key hepatic gluconeogenic enzyme, phosphoenolpyruvate carboxykinase (*Pepck*), a rate-limiting enzyme in liver and kidney gluconeogenesis, which catalyzes the conversion of oxaloacetate into phosphoenolpyruvate, was significantly downregulated in the NEMO^{LPC-KO}*Ccr2*^{-/-} mice (Figure 3E).

microscopy of liver sections from 8-week-old mice. (E) Sirius Red area quantification, (F) hepatic hydroxyproline content after 8 and 12 weeks, and (G) expression of fibrosis-related mRNA in liver tissue. (H) Hepatic tumors at the 26 weeks of age (representative macroscopic pictures of 26-week-old mice), (I) as quantified by the cumulated diameter of tumors and tumors larger than 1 mm. Data represent median of n = 3–6; *P < .05, ***P < .001 (1-way analysis of variance).



The sterol-regulatory element binding protein-2 (SREBP-2) is the master regulator of cholesterol biosynthesis. In the nucleus, mature SREBP-2 (nSREBP-2) induces the expression of numerous genes involved in cholesterol homeostasis. Interestingly, *Srebp-2* mRNA was significantly downregulated in both NEMO^{LPC-KO}*Ccr2*^{-/-} and NEMO^{LPC-KO}*Ccr5*^{-/-} mice. SREBP1 is the master regulator of lipogenesis. The mRNA that codes for the *SREBP1a*, a minor isoform of SREBP1 that is structurally very similar to SREBP-2, significantly contributes to the human hepatic SREBP1 pool.¹⁷ Inactivation of SREBP-1a phosphorylation was demonstrated to prevent fatty liver disease in mice.¹⁸ Similar to SREBP-2, also SREBP-1a induces cholesterol biosynthesis, if cholesterol levels in the cell are too low.

Peroxisome proliferator-activated receptor (PPAR) α , β / δ , and γ modulate lipid homeostasis, but are also involved in inflammation and fibrosis.¹⁹ PPAR γ stores triacylglycerol in adipocytes,²⁰ but is also involved in protecting HSCs from fibrogenic activation. Interestingly, we found that *Ppar- γ* mRNA was significantly downregulated in the NEMO^{LPC-KO}*Ccr2*^{-/-} mice (Figure 3E), which aligns well with the Oil red O staining data and implies important roles of CCR2 in hepatic steatosis.

In order to address whether the metabolic stress is related to spontaneous cell death in the different knockout mouse strains and represents a possible reason for the liver injury in the 8-week-old mice (Figure 1A), we performed TUNEL (terminal deoxynucleotidyl transferase dUTP nick end labeling) staining of cryosection from 8-week-old mice. We noted a reduction in the number of apoptotic cells by the deficiency in CCR2, whereas lack of CCR5 only led to a mild decrease compared with the liver of NEMO^{LPC-KO} mice (Figure 3F). The reduction in the number of apoptotic cells by the deficiency in CCR2 was statistically significant (Figure 3G). We further studied the expression of several genes related to cell death, the Fas ligand, which is upregulated by cells that undergo apoptosis, and MnSOD (manganese superoxide dismutase). In mammalian cells, MnSOD is a key mitochondrial antioxidant enzyme that detoxifies the free radical superoxide, the major by-product of mitochondrial respiration,²¹ and MDM2 (mouse double minute 2 homolog) is an important negative regulator of the p53 tumor suppressor. Importantly, all 3 mRNA, *FasL*, *MoSod*, and *Mdm2* were significantly downregulated in the NEMO^{LPC-KO}*Ccr2*^{-/-} mice (Figure 3H).

These data in summary demonstrate that CCR5 deficiency increased steatosis in NEMO^{LPC-KO} mice, while CCR2 deficiency partially protects from metabolic alterations, suggesting that both chemokine receptors are involved in many different cellular pathways during liver injury progression.

Impact of CCR2 or CCR5 Deficiency on Hepatocyte Viability and HSC Activation in NEMO^{LPC-KO} Mice

The chemokine receptors CCR2 and CCR5 are not expressed by hepatocytes.²² Nonetheless, we wanted to exclude that chemokine receptor deficiency would alter proliferation or viability of hepatocytes, which would explain altered tumorigenesis. Therefore, we isolated primary hepatocytes from the livers of the different mouse strains.²³ Hepatocytes isolated from all NEMO^{LPC-KO} mice showed a reduced viability in culture compared with NEMO-proficient cells, as reported previously,¹ but this was not altered by the additional deletion of CCR2 or CCR5 (Figure 4A and B).

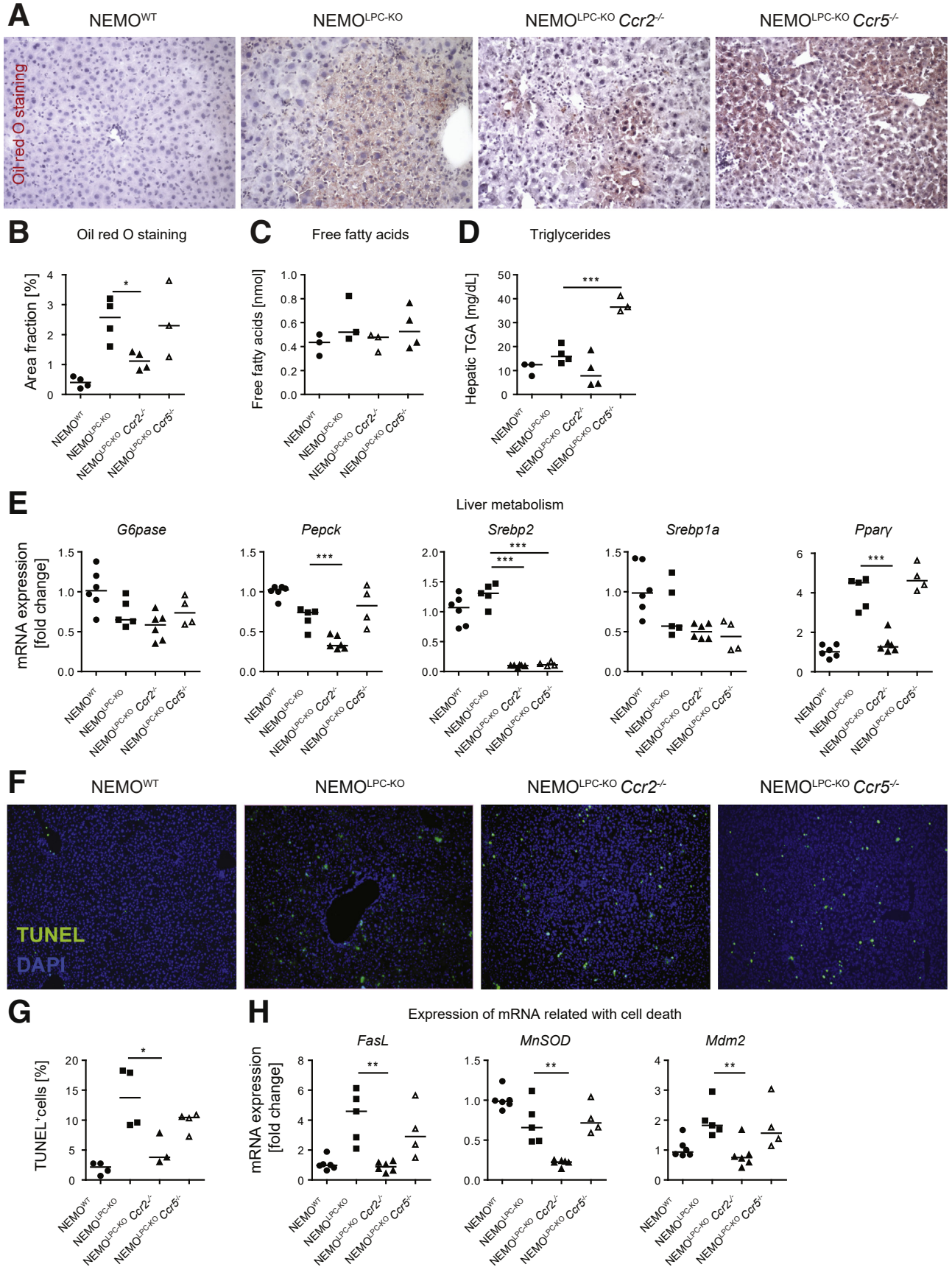
We next focused on HSCs as the key fibrogenic cell population. As CCR5 is expressed by HSC and has been convincingly linked to their activation,²⁴ we isolated HSC from WT and *Ccr5*^{-/-} mice. Cell culture micrographs demonstrated that the cells from *Ccr5*^{-/-} mice exhibited a similar morphology like those of WT mice (Figure 4C). However, when primary HSC were treated with either 100-ng/mL LPS, 25 ng/mL platelet-derived growth factor (PDGF), or 1 ng/mL of transforming growth factor beta (TGF- β), we observed a significant reduced secretion of CCL2 and IL6 by the CCR5-deficient HSC after treatment with PDGF and TGF- β (Figure 4D).

These data indicate a reduced HSC activation in CCR5-deficient mice, which includes the reduced release of inflammatory cytokines upon activating stimuli in HSC from CCR5-deficient NEMO^{LPC-KO} mice.

Role of CCR2 or CCR5 Deficiency on Hepatic Macrophage Composition and Activation in NEMO^{LPC-KO} Mice

Because we observed a pronounced infiltration of leukocytes in liver tissue (Figure 1A), we analyzed the potential contribution of different types of immune cells to liver injury in the NEMO^{LPC-KO} mice. Using immunohistochemical staining for the pan-leukocyte marker CD45, we observed that immune cells were generally increased in livers of NEMO^{LPC-KO} mice (Figure 5A), whereas additional constitutive deficiency in *Ccr2*, but not *Ccr5*, led to a slight reduction in hepatic leukocytes (Figure 5B). However, the composition of immune cells in the liver was quite strikingly affected in the different knockout animals. While NEMO^{LPC-KO} mice showed highly elevated total macrophages (as assessed by F4/80 immunohistochemistry), the additional deficiency in *Ccr2* significantly reduced their numbers. Constitutive deletion of *Ccr5*^{-/-} reduced macrophage numbers to a lesser extent but led to the formation of cell clusters (Figure 5C). CCR2 deficiency had a more pronounced effect on reducing

Figure 2. (See previous page). Effects of *Ccr2* or *Ccr5* deficiency on LPS-induced acute liver injury in NEMO LPC-deficient mice. (A) Hematoxylin and eosin stainings of liver sections from WT, NEMO^{LPC-KO}, NEMO^{LPC-KO}*Ccr2*^{-/-}, and NEMO^{LPC-KO}*Ccr5*^{-/-} mice at the age of 8 weeks that were either left untreated or challenged with LPS for 4 hours at the dose of 0.42 μ g/kg. (B) Liver injury (ALT activity) in these animals. (C) Cytokine expression in liver tissue was monitored using a multiplex assay. Data represent median of n = 3–6; **P* < .05, ****P* < .001 (1-way analysis of variance).



macrophages in liver sections (Figure 5D). Flow cytometric studies demonstrated that the elevated macrophages in NEMO^{LPC-KO} mice mostly consisted of CD11b⁺F4/80⁺ MoMF (red gate) rather than of CD11b⁻F4/80⁺ Kupffer cells (green gate, Figure 5E). The MoMF were strongly reduced in the NEMO^{LPC-KO} Ccr2^{-/-} mice compared with NEMO^{LPC-KO} mice (Figure 5F), consistent with the known function of CCR2 for recruiting monocyte-derived macrophages to injured liver.⁵ In order to study macrophage polarization in the different mouse strains, we further studied the surface expression of the polarization markers IL4 receptor α (CD124), the mannose receptor (CD206), and the C-type lectin domain family 10 member A (CLEC10A, CD301) by flow cytometry (Figure 5G). Notably, we found a reduced expression of CD124 and CD206 by all 3 types of NEMO^{LPC-KO} mice, whereas CD301 expression was slightly elevated by the NEMO^{LPC-KO} Ccr2^{-/-} mice and NEMO^{LPC-KO} Ccr5^{-/-} mice (Figure 5H). These data emphasize the profound impact of CCR2 and CCR5 deficiency of hepatic macrophage numbers as well as their polarization.

Role of CCR2 or CCR5 Deficiency on Lymphocyte Populations in NEMO^{LPC-KO} Mice

Lymphocytes are particularly important in limiting or supporting hepatocarcinogenesis.²⁵ The natural killer (NK) cells, which can eliminate tumor cells, were strongly reduced in NEMO^{LPC-KO} mice, but higher in NEMO^{LPC-KO} Ccr2^{-/-} mice (Figure 5I). Cytotoxic CD8 T cells were significantly increased in all in NEMO^{LPC-KO} mouse strains, while CD4 T cells were lower in livers of in NEMO^{LPC-KO} mice (Figure 5J).

Functional Differences of Macrophage Subsets in NEMO^{LPC-KO} Mice

In order to understand the functional implications of reduced MoMF in comparison with KC in NEMO^{LPC-KO} mice, we isolated MoMFs and KCs by fluorescence-activated cell sorting from the livers of NEMO^{WT} and NEMO^{LPC-KO} mice to assess the expression of selected mRNAs related to inflammatory activation and cell killing activity. Interestingly, the KCs but not the MoMFs upregulated TNF in NEMO^{LPC-KO} mice. TNF is considered the main trigger for hepatocyte apoptosis in NEMO-deficient LPCs.¹ Similarly, KCs upregulated IL1 β . On the contrary, TRAIL (TNF-related apoptosis-inducing ligand) or FasL as potential pathways of inducing cell death in hepatocytes were nearly unaffected in both macrophage subsets. The anti-inflammatory IL10, the prototypic anti-inflammatory cytokine, was upregulated in the MoMF as well as in KC (Figure 6A). These data imply important functional differences between MoMF and KC in NEMO^{LPC-KO} mice.

We had previously demonstrated that CCR5 expression is dispensable for monocyte recruitment in liver injury,²⁶ supporting that the effects on hepatic macrophage numbers in NEMO^{LPC-KO} Ccr5^{-/-} mice reflect adapted responses, for instance, due to reduced CCL2 release by HSC (Figure 4C). However, because monocytes and macrophages can express CCR5, we next assessed whether macrophage functions would be altered in CCR5-deficient mice. To this end, bone marrow-derived macrophages (BMDMs) were generated in culture for 7 days and then stimulated with 20-ng/mL IL4 or with 100-ng/mL IFN γ for 24 hours to assess M1- or M2-type responses, respectively.²⁷ Interestingly, IL1 β expression was increased in BMDM from Ccr5^{-/-} compared with WT mice. Further, Ccr5 deficiency led to increased expression of TNF after stimulation with IFN γ . Stimulation of BMDM from the Ccr5^{-/-} mice with IL4 led a significant elevation of FasL expression, and stimulation with IFN γ similarly led to strongly increased expression (Figure 6B). Collectively, these data support that CCR2 was important for macrophage recruitment in NEMO^{LPC-KO} mice, while CCR5 affected their inflammatory activation.

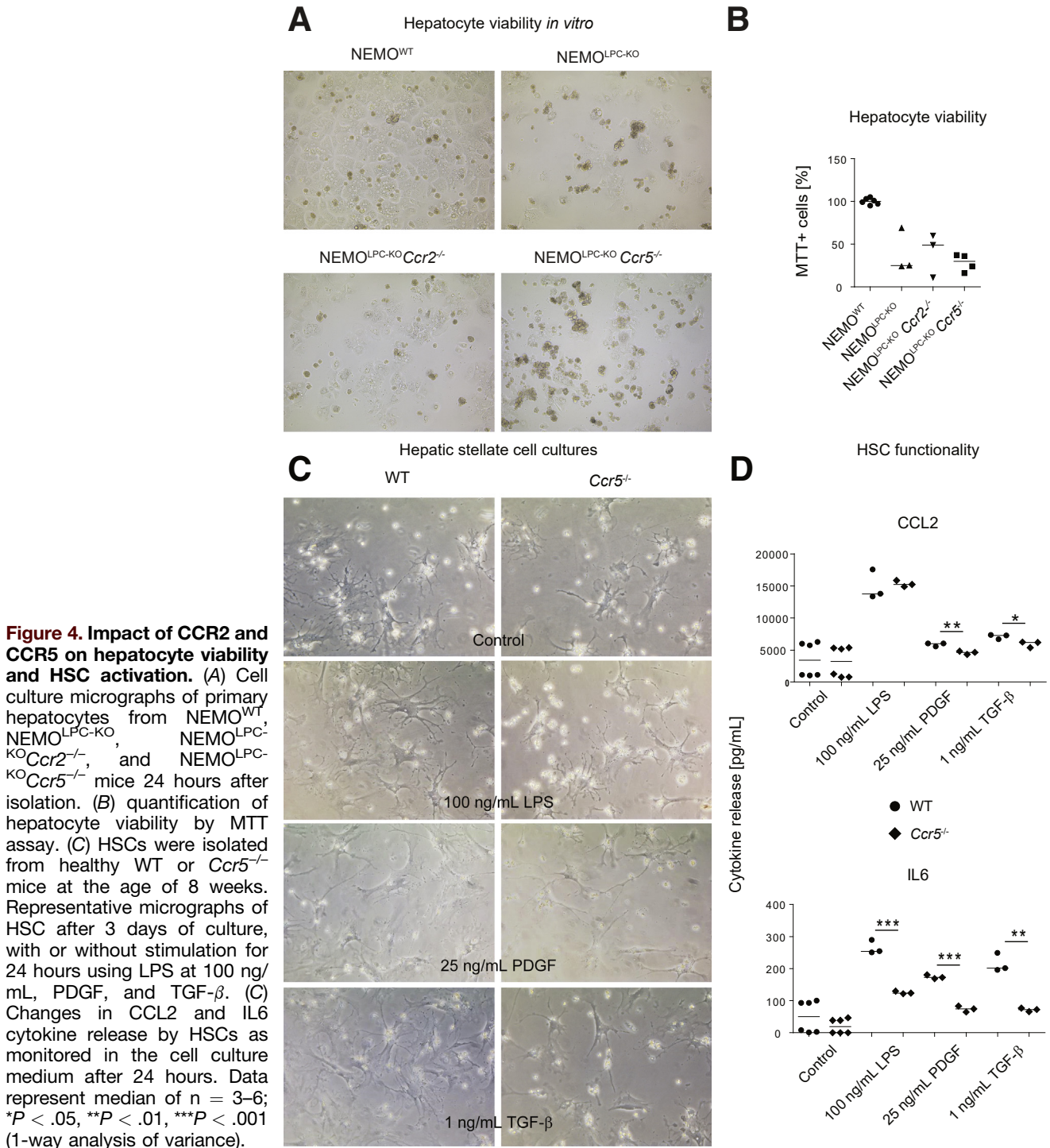
Impact of CCR2 or CCR5 Deficiency on Circulating Leukocytes in NEMO^{LPC-KO} Mice

Changes in the intrahepatic immune cell composition were partially reflected by circulating myeloid and lymphoid cells in the blood, which were simultaneously assessed by flow cytometry.²⁷ We observed similar monocyte numbers in NEMO^{LPC-KO} mice as in WT mice, whereas monocytes were reduced in NEMO^{LPC-KO} Ccr2^{-/-} and NEMO^{LPC-KO} Ccr5^{-/-} mice (Figure 7A and C). Interestingly, there was a shift toward Ly6C^{high} monocytes in NEMO^{LPC-KO} and was less pronounced in NEMO^{LPC-KO} Ccr2^{-/-} mice, whereas Ly6C^{low} and Ly6C^{high} subpopulations appeared similarly frequent in WT and NEMO^{LPC-KO} Ccr5^{-/-} mice (Figure 7B). Moreover, neutrophils were significantly reduced in NEMO^{LPC-KO} Ccr5^{-/-} mice (Figure 7C). Natural killer cells were strongly reduced in the blood of the NEMO^{LPC-KO} and NEMO^{LPC-KO} Ccr2^{-/-} mice, whereas their numbers in NEMO^{LPC-KO} Ccr5^{-/-} mice were similar to those of WT mice (Figure 7D and E).

Functional Contribution of Lymphocyte Subsets and Macrophages to Liver Injury in NEMO^{LPC-KO} Mice

In order to link the changes in lymphocyte and macrophages numbers observed in NEMO^{LPC-KO} Ccr2^{-/-} and NEMO^{LPC-KO} Ccr5^{-/-} mice to the altered disease phenotype in the NEMO^{LPC-KO} model, we selectively depleted different cell populations in NEMO^{LPC-KO} mice and assessed the consequences on liver injury. We opted for

Figure 3. (See previous page). Effects of Ccr2 or Ccr5 deficiency on liver metabolism and cell death in NEMO LPC-deficient mice. Eight-week-old WT, NEMO^{LPC-KO}, NEMO^{LPC-KO} Ccr2^{-/-}, and NEMO^{LPC-KO} Ccr5^{-/-} mice were analyzed for (A) steatosis using Oil red O staining. (B) Oil red O quantifications. (C) Analysis of free fatty acids from liver tissue. (D) Assessment of triglycerides levels from liver tissue. (E) Expression of metabolism-related mRNA in liver tissue. (F) TUNEL staining for apoptotic cell death and (G) quantification. (H) Expression of selected mRNA related to cell death. Data represent median of n = 3–7; *P < .05 (1-way analysis of variance).



antibody-based depletion to ensure an inducible, rapid, transient, and highly specific immune cell reduction. Upon administration of a CD8 T cell-depleting antibody, intrahepatic CD8 T cells were reduced by about 60% in the liver and more potently depleted in the circulation. CD8 T cell reduction/depletion did not significantly affect ALT levels in NEMO^{LPC-KO} mice (Figure 8A). Similarly, NK cells were effectively reduced in the liver by a depleting

antibody, but did not significantly reduce liver injury either (Figure 8B). In order to study the broader inhibition of different immune cells at the same time, we administered dexamethasone, a potent corticosteroid with anti-inflammatory activity, at a concentration of 1-mg/kg body weight intravenously to NEMO^{LPC-KO} mice. Dexamethasone slightly improved liver histology (and notably reduced ALT levels (Figure 8C).

Unexpectedly, the depletion of Gr1 positive cells (ie, monocytes or macrophages and neutrophils) led to a significant elevation of “spontaneous” liver injury in NEMO^{LPC-KO} mice (Figure 9A). CLLs eliminate all macrophages after intravenous injection as shown by flow cytometric quantification of the hepatic F4/80⁺ cells using flow cytometry (Figure 9B), and F4/80 using immunohistochemistry (Figure 9C). Unexpectedly, the CLLs also dramatically increased liver injury in NEMO^{LPC-KO}, NEMO^{LPC-KO}*Ccr2*^{-/-}, and particularly in NEMO^{LPC-KO}*Ccr5*^{-/-} mice but not in NEMO^{WT} mice (Figure 9D).

The CLL-mediated macrophage depletion prompted the significant induction of CCL2, the signal for monocytes to emigrate from the bone marrow and replenish the depleted macrophages, while there were no effects on TNF, CCL3, or other cytokines (Figure 9E). The tissue injury in liver was specifically pronounced in the NEMO^{LPC-KO}*Ccr5*^{-/-} mice, with hemorrhages apparent after 16 hours, which became reduced after 40 hours (Figure 9F). Interestingly, the liver injury (by histology) and ALT levels rapidly declined within 2 days after CLL (Figure 9F and G), along with the repopulation of macrophages in the liver after CLL depletion (data not shown).

Altogether, these experiments pointed toward an important tissue-protecting role of macrophages, particularly on the CCR5-deficient background, while the extent of liver injury appeared not immediately modulated by CD8 T or NK cells.

CCR5⁺ Macrophages Limit Liver Injury in NEMO^{LPC-KO} Mice

NEMO^{LPC-KO}*Ccr5*^{-/-} mice were characterized by increased spontaneous liver injury, higher steatosis and increased incidence of liver cancer (Figure 1), which was accompanied by altered macrophage functionality (Figure 6) and increased injury upon macrophage depletion (Figure 9). We used the model of aggravated liver injury in NEMO^{LPC-KO}*Ccr5*^{-/-} mice upon CLL-mediated macrophage depletion to test the specific roles of immune cells for limiting liver damage. Therefore, CLL-treated NEMO^{LPC-KO}*Ccr5*^{-/-} mice were subjected to adoptive cell transfers, using mature macrophages (BMDMs), immature bone marrow monocytes (CD115⁺), or as a control cell population, B cells from spleen (Figure 10A).

Adoptively transferred BMDMs were labelled with fluorescent latex microparticles to track their distribution and differentiation. Injection of 2 million BMDMs corresponded to about 7% fluorescent positive blood leukocytes (Figure 10B), whereas huge cell numbers migrated into the liver with about 5% fluorescent positive hepatic leukocytes, of which most were F4/80⁺ and showed markers of both MoMFs and KCs (Figure 10C). The successful accumulation of the transferred cells in the injured liver principally support the concept of macrophage-based cell therapies to limit liver disease progression.²⁸ Interestingly, BMDMs significantly reduced the massive liver injury induced by CLLs in NEMO^{LPC-KO}*Ccr5*^{-/-} mice, while immature monocytes (CD115⁺) and B cells only mildly reduced liver injury, as reflected by liver histology (Figure 10D) and ALT levels (Figure 10E).

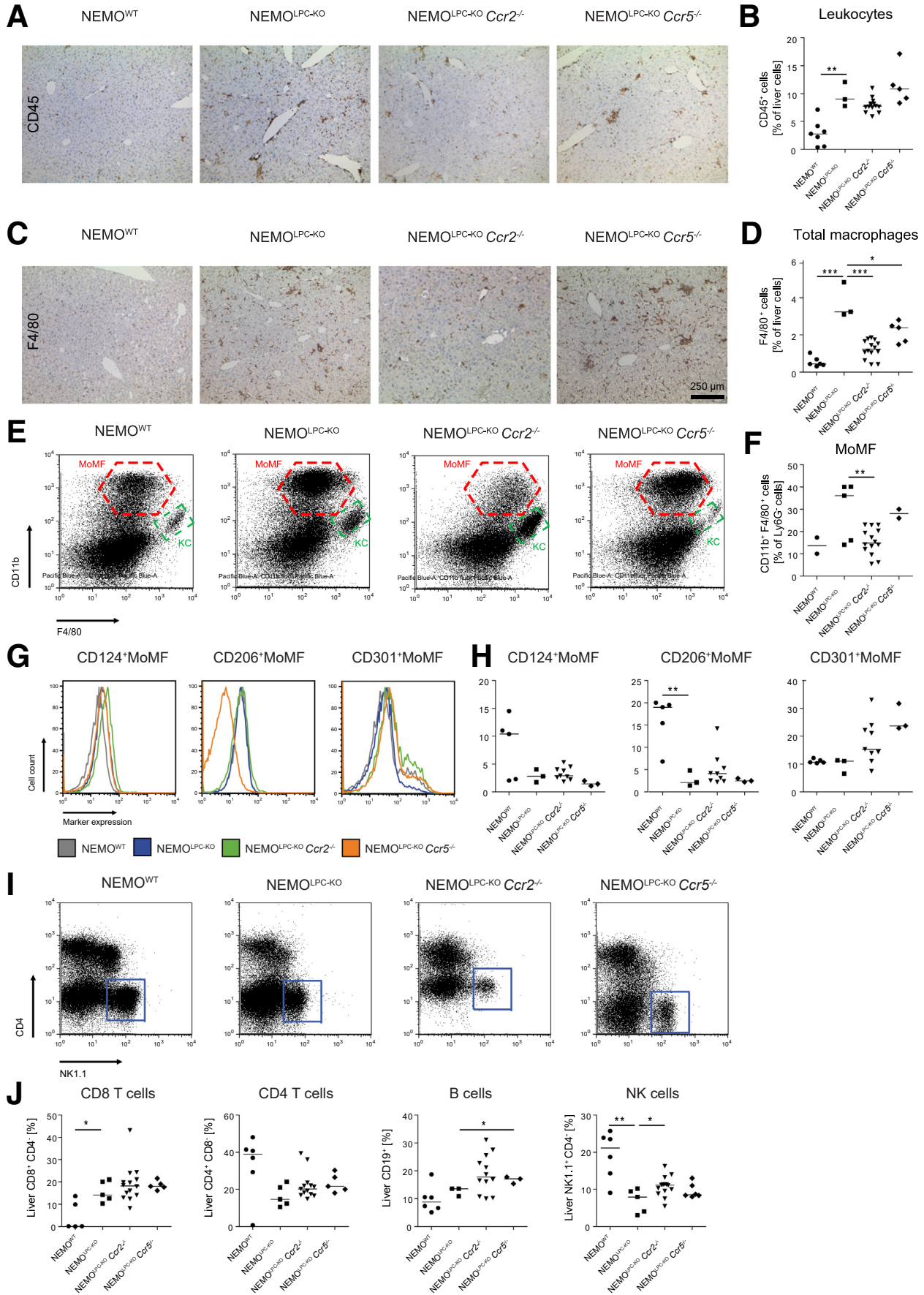
Our data thus suggest that macrophages play an important regulatory role in liver injury, which is particularly associated with CCR5.

Discussion

The dual inhibition of CCR2 and CCR5 by cenicriviroc is a strategy, which is currently undergoing clinical trials in NASH patients, including the phase 3 AURORA trial (Allergan, South San Francisco, CA). Nevertheless, there are still open issues on cenicriviroc such as the durability of anti-fibrotic responses, divergent effects on NASH vs fibrosis, potential long-term concerns and the expected path to approval.¹⁰ While cenicriviroc inhibits both chemokine receptors, we have studied the individual roles of both receptors during different stages of chronic liver diseases.¹ Our data from the NEMO^{LPC-KO} mice support the existing data on the role of CCR2 for the recruitment of MoMF into liver and its beneficial impact on fibrosis.⁸ Unexpectedly, this deficiency of hepatic MoMF led to increased liver injury, similar to the impact of CCR5 deficiency, which significantly enhanced liver injury at the time point of 8 weeks.

The chemokine receptor CCR2 is known as an important regulator of myeloid cell migration. We have shown before that deficiency in CCR2 leads to reduced inflammation and fibrosis in liver fibrosis.⁸ Yet, the CCL2-CCR2 axis is not limited to the liver, but is important for the migration of monocytes into other organs as well. Moreover, recent studies suggest that the importance of CCL2 is not just limited to functioning as a chemoattractant, but that it affects various cellular processes, such as leukocyte polarization, secretion of effector molecules, autophagy, killing, and survival.²⁹ Furthermore, our study indicates that CCR2 might also be involved in the regulation of cell death and oxidative stress. In the NEMO^{LPC-KO} and the NEMO^{LPC-KO}*Ccr5*^{-/-} mice, Mdm2 is upregulated and thus, it is very likely that it thereby inhibits p53 expression, an important tumor suppressor, and consequently accelerates tumor growth in WT mice.³⁰

However, the significantly increased liver injury observed in the NEMO^{LPC-KO}*Ccr2*^{-/-} mice apparently cannot be led back to the effects on cell death. Importantly, CCR2 and CCL2 have been shown to not only promote inflammation and putative organ damage, but they have also support healing and regeneration. It is thus apparent that also CCR2 might be another double-edged sword: while it amplifies inflammation,⁸ it is also involved in the resolution of liver fibrotic scars, as presented previously.³¹ There are several examples for protective functions of CCL2 and CCR2. CCL2 promotes healing in diabetic wounds by restoring the macrophage response.³² In addition, CCR2 shows immunomodulatory and protective effects during central nervous system inflammation and promotes protective microglial accumulation in early stages of Alzheimer's disease.³³ In line, our data show that the NEMO^{LPC-KO}*Ccr2*^{-/-} mice not only downregulate inflammatory mediators such as *Thf*, *Il1*, and *Il6*, but also anti-inflammatory *Il10* and *Tgf-β*, indicating a reduction in markers associated with healing and downregulation of inflammation as a consequence of CCR2 deficiency.



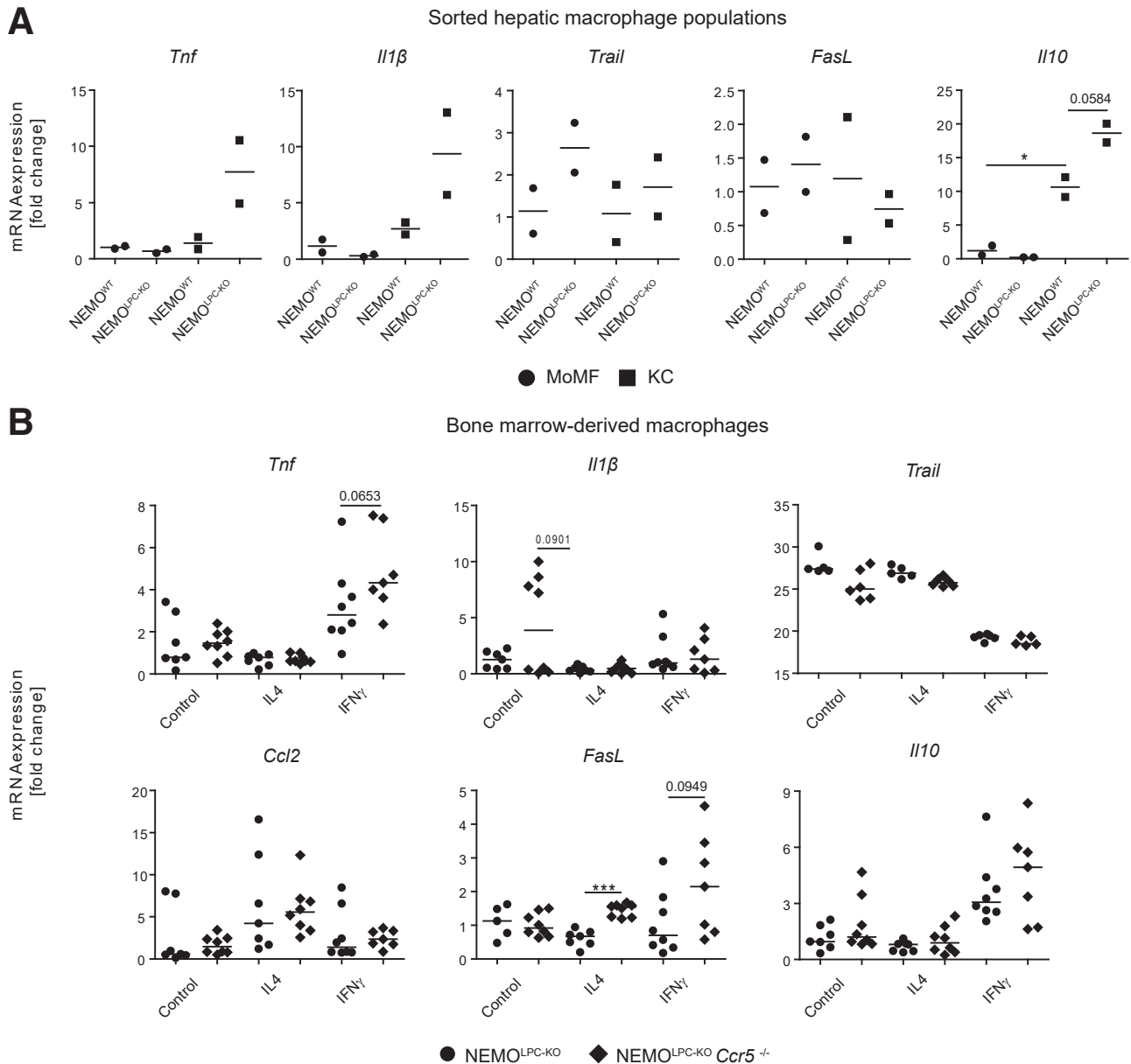
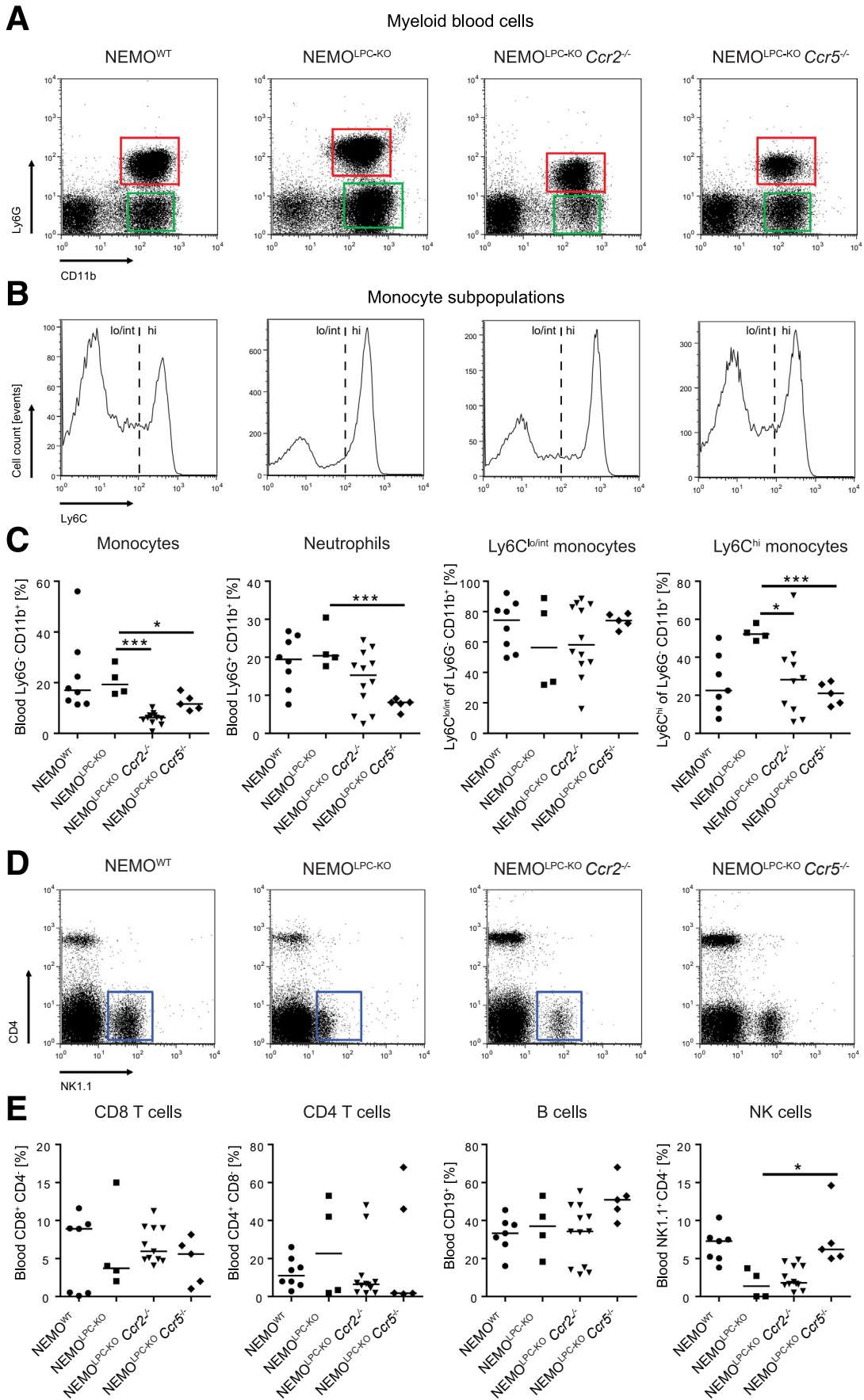


Figure 6. Role of hepatic macrophage subsets and effects of *Ccr5* deficiency on macrophage activation in NEMO LPC-deficient mice. (A) Hepatic macrophage subsets (CD11b⁺F4/80^{int} monocytic macrophages and CD11b^{int}F4/80⁺ KCs) were sorted from livers of 8-week-old NEMO^{WT} and NEMO^{LPC-KO} mice, and mRNA expression of inflammatory cytokines and markers was quantified using real-time quantitative polymerase chain reaction. (B) BMDMs were generated from 8-week-old NEMO^{LPC-KO} and NEMO^{LPC-KO} *Ccr5*^{-/-} and cultured for 6 days, followed by 24 hours of stimulation with 20-ng/mL IL4, or IFN γ , and mRNA expression of inflammatory markers was analyzed using quantitative real-time polymerase chain reaction. Data represent median of n = 2–6; **P* < .05, ****P* < .001 (1-way analysis of variance).

Figure 5. (See previous page). Effects of *Ccr2* or *Ccr5* deficiency on hepatic immune cell infiltration in NEMO LPC-deficient mice. NEMO^{LPC-KO}, NEMO^{LPC-KO} *Ccr2*^{-/-}, and NEMO^{LPC-KO} *Ccr5*^{-/-} mice were analyzed at the age of 8 weeks. (A) Immunohistochemical staining of the pan-leukocyte marker CD45 and (B) quantification of liver leukocytes by flow cytometry. (C) Macrophage staining based on F4/80 and (D) quantification of liver macrophages by flow cytometry. (E) Analysis of hepatic macrophage subsets, mainly CD11b⁺F4/80^{int} monocytic macrophages (MoMF, red gate) and CD11b^{int}F4/80⁺ KCs (green gate), and (F) quantification of MoMFs. (G) Flow cytometric analysis of markers of alternative macrophage activation expressed by MoMFs, and (H) quantifications thereof. (I) Representative flow cytometric plots of hepatic lymphoid cells (blue gate: NK cells), and (J) statistical summary of cell frequencies. Data represent median of n = 2–14; **P* < .05, ***P* < .01, ****P* < .001 (1-way analysis of variance).



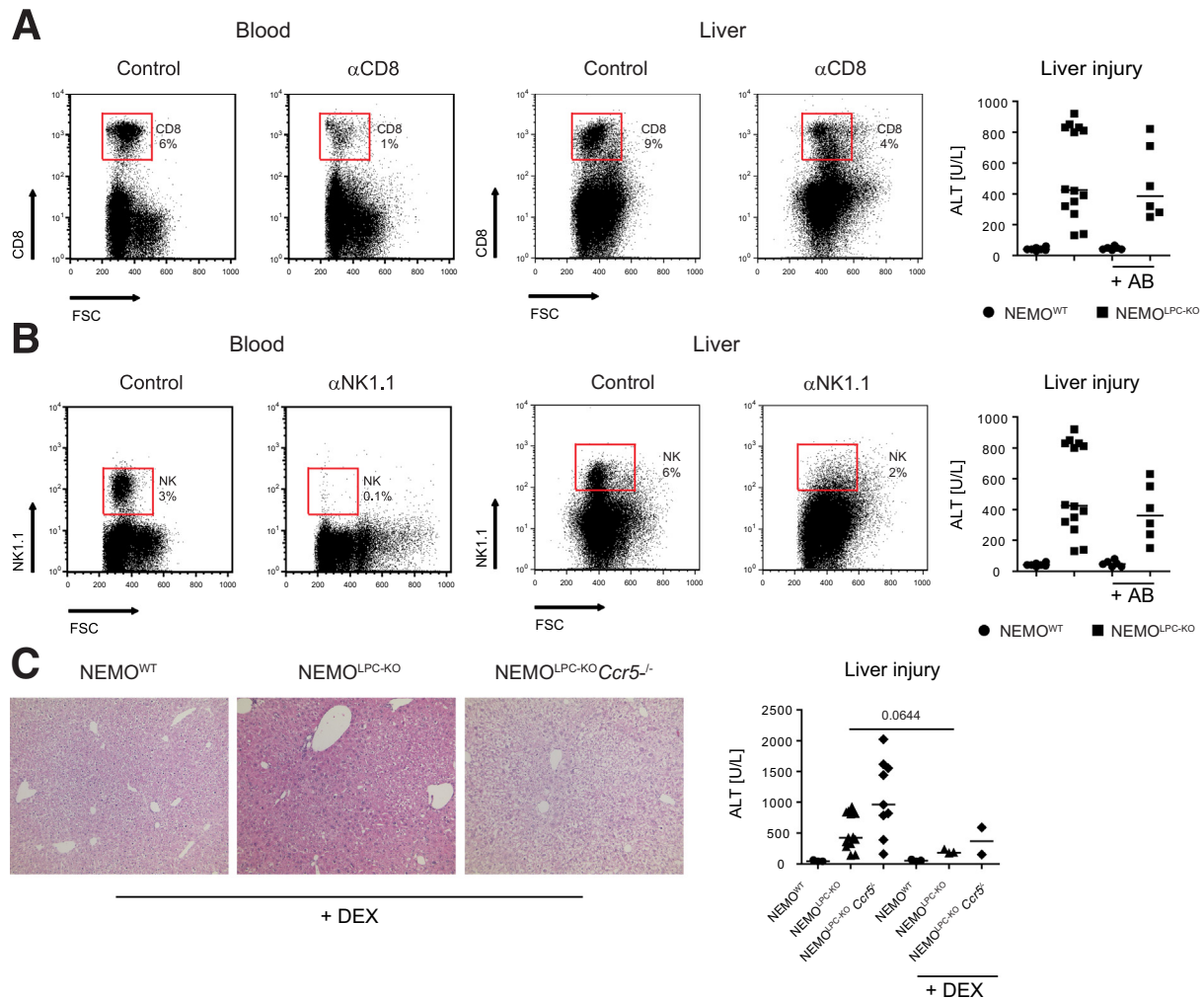


Figure 8. Roles of lymphoid immune cell subsets for liver injury in NEMO parenchymal cell-deficient mice. Specific lymphoid immune cell subsets were depleted in vivo using monoclonal antibodies in NEMO^{WT}, NEMO^{LPC-KO}, NEMO^{LPC-KO} Ccr2^{-/-}, and NEMO^{LPC-KO} Ccr5^{-/-} mice at the age of 8 weeks. (A) Treatment with 100 μ g of anti-CD8 antibody (clone TIB 210) reduces CD8⁺ T cells (representative fluorescence-activated cell sorting plots from peripheral blood and liver, 24 hours after monoclonal antibody injection), but does not affect liver injury (depicted as ALT levels, 24 hours after monoclonal antibody injection). (B) Reduction of NK and NK T cells by 100- μ g anti-NK1.1 antibody (clone PK136) in blood and liver after 24 hours. (C) Effects of 1 mg/kg body weight dexamethasone (DEX) on liver injury. Data represent median of n = 4–6 \pm SD; *P < .05, ***P < .001 (1-way analysis of variance). FSC, forward scatter.

In our study, we have observed that the liver injury strongly declines in the 12-week-old mice while it was significantly elevated at the age of 8 weeks. This suggests a stage-dependent process of inflammation. Interestingly, dermatological research has demonstrated that a depletion of macrophages at early stage of the skin repair response (inflammatory phase) significantly reduced the formation of vascularized granulation tissue, impaired epithelialization, and resulted in minimized scar formation. In contrast, and most importantly, when macrophages are depleted at a middle stage of the skin repair response, hemorrhages

appear in the wound tissue. Finally, macrophage depletion restricted to the late stage of repair did not affect the outcome of the repair response.³⁴

Therefore, the spontaneous liver injury in the NEMO^{LPC-KO} Ccr2^{-/-} mice can very likely be explained by the reduction in CCR2⁺ macrophages that also function in wound healing and tissue regeneration, and also by a time-dependent function of monocytes and macrophages that differs at early-term and midterm stages (the 8-week-old mice in our study representing the early term and the 12-week-old mice the midterm stage).

Figure 7. (See previous page). Effects of Ccr2 or Ccr5 deficiency on myeloid and lymphoid blood cells in NEMO^{LPC-KO} mice. NEMO^{WT}, NEMO^{LPC-KO}, NEMO^{LPC-KO} Ccr2^{-/-}, and NEMO^{LPC-KO} Ccr5^{-/-} mice at the age of 8 weeks were analyzed for immune cell subsets in blood using flow cytometry. (A) Representative flow cytometric plots, (B) histograms of Ly6C expression on blood monocytes, and (C) statistical summary of cell frequencies. (D) Representative flow cytometric plots of lymphoid blood cells, and (E) statistical summary of cell frequencies. Data represent median of n = 4–14 \pm SD; *P < .05, ***P < .001 (1-way analysis of variance).

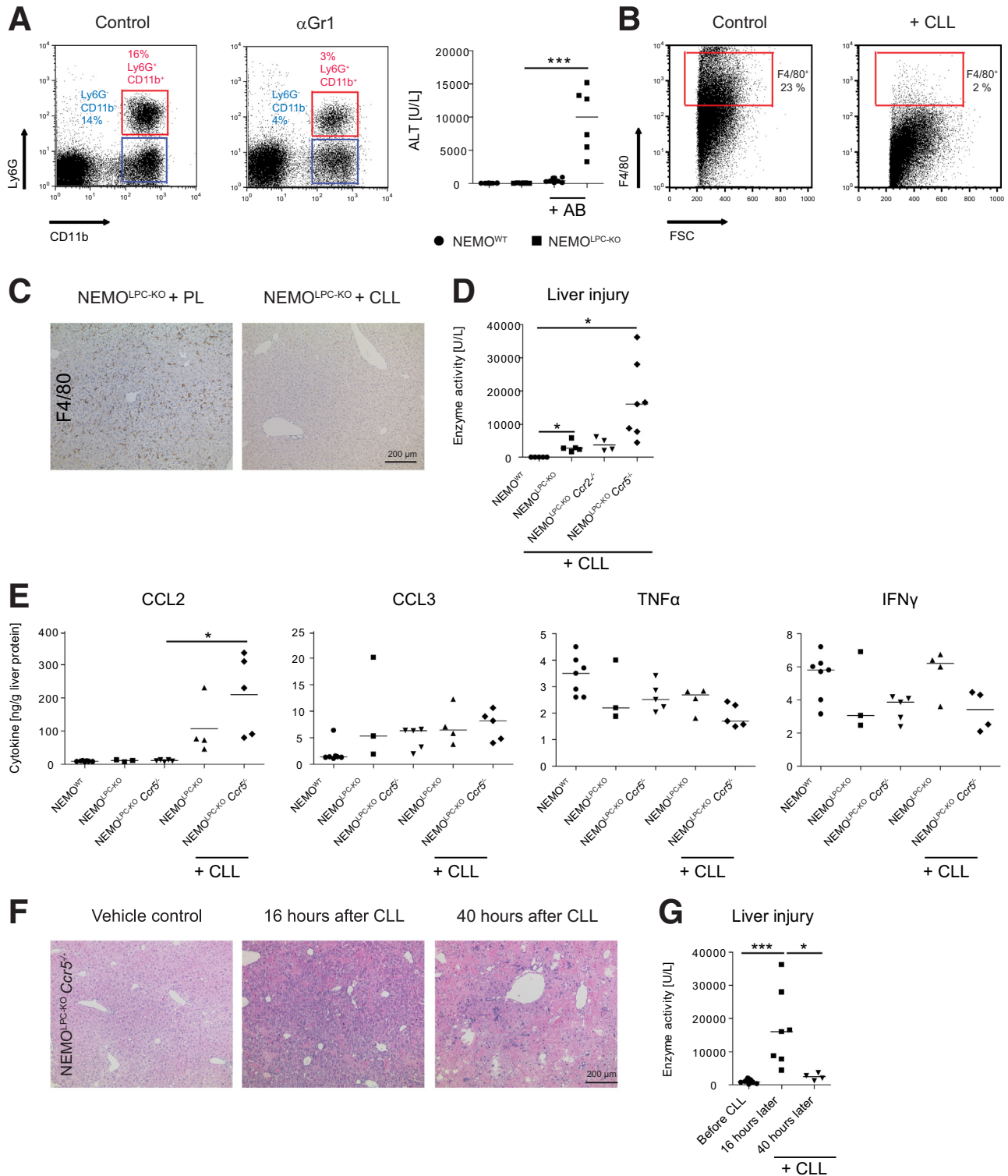


Figure 9. Functional role of myeloid immune cells for modulating liver injury in NEMO-LPC-deficient mice. Specific immune cell subsets were depleted in vivo using monoclonal antibodies or macrophage-depleting CLL in WT, NEMO^{LPC-KO}, NEMO^{LPC-KO} Ccr2^{-/-}, and NEMO^{LPC-KO} Ccr5^{-/-} mice at 8 weeks of age. (A) Reduction of CD11b⁺ myeloid cells by 100 μ g of the antibody RB6-8C5 significantly increased liver injury in NEMO^{LPC-KO} mice as shown by flow cytometry. (B) CLLs led to a potent depletion of F4/80⁺ cells in the liver as shown by flow cytometry and (C) F4/80 immunohistochemistry. (D) CLLs significantly increased hepatic injury in NEMO^{LPC-KO}, NEMO^{LPC-KO} Ccr2^{-/-}, and NEMO^{LPC-KO} Ccr5^{-/-} mice. (E) Effects of CLLs on selected hepatic cytokines. (F) Liver histology of NEMO^{LPC-KO} Ccr5^{-/-} mice during the time course of CLL-mediated macrophage deletion. (G) Corresponding ALT levels. Data represent median of n = 3–7 \pm SD; *P < .05, ***P < .001 (1-way analysis of variance).

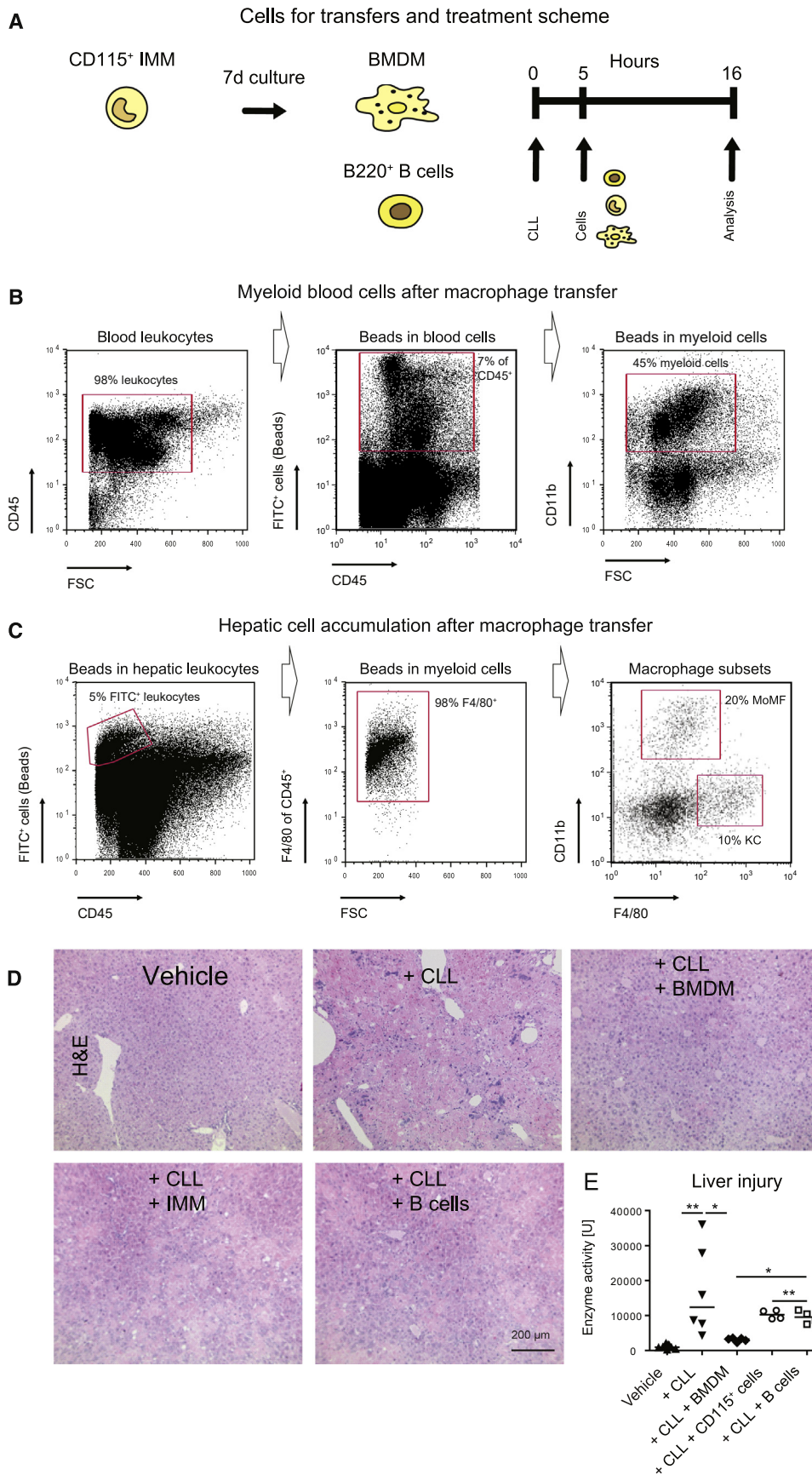


Figure 10. Amelioration of liver injury in $NEMO^{LPC-KO} Ccr5^{-/-}$ mice with adoptive macrophage cell transfer. $NEMO^{LPC-KO} Ccr5^{-/-}$ mice at the age of 8 weeks were treated with CLLs and received 5 hours later $CD115^{+}$ cells from bone marrow (immature monocytes [IMMs]), B cells (from spleen), and BMDMs. Mice were sacrificed after another 11 hours. (A) Experimental setup for adoptive cell transfer. (B) In blood, 7% of $CD45^{+}$ leukocytes were $FITC^{+}$, and the majority (45%) were myeloid cells. (C) Bead-bearing cells accumulated in liver with 5% of liver leukocytes containing beads. The $FITC(beads)^{+}$ cells at 98% $F4/80^{+}$ macrophages (middle graphics) showed either markers of $CD11b^{+} F4/80^{int}$ monocytic macrophages (MoMFs) or $F4/80^{+} CD11b^{-}$ (KCs). (D) Liver histology after the cell transfers and (E) corresponding ALT levels as a measure of liver injury in the different treatment conditions. Data represent median of $n = 4-6 \pm SD$; * $P < .05$, ** $P < .01$, *** $P < .001$ (1-way analysis of variance).

Liver metabolism is a major reflector of obesity, and expression of key genes of metabolism can help to understand the grounds of NAFLD development. Here, we not only demonstrate for the first time that CCR2 is involved in cellular migration and inflammatory activation, but also, according to the data, suggest that CCR2 may trigger the expression of key genes of liver metabolism, particularly PPAR γ , which was downregulated in the CCR2-deficient mice. PPAR γ has distinct roles in different tissues and cell types. Hepatic expression levels of PPAR γ are significantly increased in patients with NAFLD.³⁵

The role of CCR2 in liver cancer has been studied before. The CCR2 antagonist RDC018 (GSK) was shown to suppress liver tumor growth and postsurgical recurrence in subcutaneous liver tumor models.³⁶ Similarly, CCL2-neutralizing antibodies have been used to block the CCL2-CCR2 axis in mice deficient in miR-122, which develop tumors spontaneously.³⁷ Nevertheless, also the risks of targeting CCR2 in tumor therapy have been identified. Eggert et al⁶ have shown that the functions of CCR2⁺ myeloid cells depend on the developmental stage of liver tumors. Precancerous senescent hepatocytes produce CCL2, which attracts macrophages that eliminate those precancerous lesions ("antitumoral effects"), while established hepatocellular carcinomas can also attract monocytic macrophages, which then can block antitumor activity of NK cells (tumor-promoting effects).⁶ Our own recent studies on blocking CCL2 by an RNA aptamer have demonstrated that the inhibition of CCL2 in a model of endogenous liver cancers in fibrotic livers primarily reduced tumor vascularization, rather than reducing tumor burden.⁷ The data of the study of Eggert et al⁶ indicate that, similarly to CCR5, there might be only subgroups of patients with hepatocellular carcinoma that would benefit from CCR2-directed therapy.

While a potentially almost unexplored dual role of CCR2, likewise a contribution to the resolution of inflammation might impact the outcome of liver injury, we hypothesize a different reason for the increased spontaneous liver injury in the NEMO^{LPC-KO} Ccr5^{-/-} mice. It is hypothesized that CCR5 critically affects macrophage polarization: we noticed that the mice of this genetic phenotype exhibited lower numbers of alternatively activated MoMFs that express markers of alternative activation such as CD124 und CD206. The reduced expression of these alternative activation markers might lead to an aggravation of inflammation mediated by TNF because alternatively activated macrophages downregulate inflammation. Furthermore, macrophage cultures from these mice demonstrated higher expression of *Tnf* in vitro by untreated bone marrow macrophages from Ccr5^{-/-} mice.

The reduction of fibrosis in NEMO^{LPC-KO} Ccr5^{-/-} mice is most likely related to a reduced activation of HSCs, which we have observed in vitro with isolated HSCs from CCR5-deficient mice in comparison with wild-type mice. The constitutive knockout of CCR5 reduces HSC activation and leads to a lower level of secreted cytokines such as CCL2 or IL6, which was also reported in the context of *Schistosoma*-infected mice.³⁸

It was shown previously that blocking CCR5 induces antitumoral macrophage polarization, and anti-CCR5 therapy was reported to be efficient in treating metastases.³⁹

Similarly, maraviroc, a CCR5 antagonist, was shown to prevent the development of hepatocellular carcinoma in a mouse model.⁴⁰ Therefore, the increased hepatocarcinogenesis, which we observed in the NEMO^{LPC-KO} Ccr5^{-/-} mice, was unexpected and may point toward a specific role of CCR5 in the model of NEMO^{LPC-KO}. In line, deletion of CCL5, the main ligand of CCR5, in NEMO^{LPC-KO} mice resulted in diminished hepatocyte apoptosis, compensatory proliferation, and fibrogenesis as a consequence of reduced immune cell infiltration.⁹ Our data indicate that the aggravated tumor phenotype in NEMO^{LPC-KO} Ccr5^{-/-} mice might be related to the altered macrophage activation, as the tumor development was observed alongside excessive injury and steatohepatitis. Therefore, not all patients might profit from a CCR5-directed tumor therapy.

Macrophage cell therapy was proposed as a potential novel curative option for liver disease.⁴¹ In a mouse model of liver fibrosis, the adoptive transfer of differentiated macrophages from bone marrow promoted regression from fibrosis. Transferred cells as well as endogenous mobilized cells upregulated matrix metalloproteinases-13 and -9, IL10, colony stimulating factor-1, insulin-like growth factor-1, and vascular endothelial growth.⁴² These data emphasize that hepatic macrophages should not simply be viewed as inflammatory cells, but rather have the capacity to modulate and restrict inflammatory processes. This appears to be particularly relevant in an inflammatory cancer model such as the NEMO^{LPC-KO} mouse model, in which the intimate interplay between TNF-releasing macrophages and TNF-susceptible NEMO-deficient hepatocytes is tightly orchestrated by the chemokine receptors CCR2 and CCR5, ultimately defining the extent of liver injury, fibrosis, and hepatocarcinogenesis.

Materials and Methods

Mice

WT, NEMO^{LPC-KO}, NEMO^{LPC-KO} Ccr2^{-/-}, and NEMO^{LPC-KO} Ccr5^{-/-} mice were housed under specific pathogen-free conditions. All experiments were performed with male mice, have been approved by the appropriate authorities according to German legal requirements, and were carried out in accordance with the EU Directive 2010/63/EU for animal experiments. The mice numbers were restricted for some experiments by the legal authorities. Group sizes were not increased once significance was reached. The NEMO^{LPC-KO} mice carry loxP-site-flanked (floxed) alleles of the Nemo gene (NemoFl) and were crossed to Alfp-Cre transgenic mice to generate a LPC-specific KO of NEMO.^{1,43} Genotypes were confirmed via polymerase chain reaction specific for the respective alleles using DNA from tail or ear biopsies.

Treatment With Dexamethasone and Induction of LPS-Induced Acute Liver Injury

Mice were treated with 1-mg/kg body weight of dexamethasone by intravenous injection. Conditioned liver injury was induced by LPS (Sigma-Aldrich, St Louis, MO) by intraperitoneal injection of 0.42 μ g/g of mouse body weight.

The NEMO^{LPC-KO} leads to a strongly increased sensitivity to cell death induction of LPCs.¹ Mice were sacrificed 4 hours after LPS injection.

Liver Enzymes, Hydroxyproline Quantification, Histology, and Immunohistochemistry

Aspartate aminotransferase and ALT enzyme activities were measured (UV test at 37°C) in serum (Roche Modular pre-analytics system; Roche Diagnostics, Rotkreuz, Switzerland). The hepatic hydroxyproline content (reflecting total intrahepatic collagen) was measured as described before.⁸ Conventional hematoxylin and eosin, Oil red O, and Sirius Red staining were performed according to established protocols.⁴⁴ Liver sections from paraffin were immunohistochemically stained for CD45, F4/80, or α SMA, as published previously.²⁷

Measurement of Hepatic Triglycerides and Free Fatty Acids

Hepatic triglycerides were assessed using the triglycerides liquicolor mono GRO-PAP Method Enzymatic Colorimetric Test for Triglycerides with Liquid Clearing Factor (Human GmbH, Wiesbaden, Germany). We used a homogenization buffer made of 78-mg Tris, 22-mg EDTA, and 4.27-g sucrose, which were resolved in 50 mL of H₂O. Liver pieces of approximately 20 mg were excised and lysed in 1000 μ L of the homogenization buffer and homogenized using a Retsch Mill (Retsch, Düsseldorf, Germany) for 1 minute at 20,000 rcf and subsequently centrifuged for 10 minutes at 3000 rcf. The supernatant was transferred into new reaction vials. The assay was performed in a 96-well plate as recommended by the manufacturer.

Free fatty acids were determined using the Free Fatty Acid Quantification Kit (Abcam, Berlin, Germany). In order to prepare liver pieces of 20 mg, an extraction buffer of 14-mL chloroform and 140- μ L Triton X-100 was prepared. 400 μ L of the extraction buffer were added to every sample which was then homogenized in a Retsch Mill for 4 minutes at a frequency of 25 rotations/min. Subsequently, samples were centrifuged for 10 minutes at 3000 rcf. A total of 200 μ L of the organic phase (lower phase) were removed from every sample and heated on a thermomixer (Eppendorf, Wesseling-Berzdorf, Germany) for 50°C, 500 rpm for 1 hour. Samples were analyzed as suggested by the manufacturer.

Cell Isolation, Culture, Transfer, and Stimulation

Bone marrow cells were isolated from murine femur and tibia, as published previously.²⁷ Immature monocytes were isolated from bone marrow, and B cells were isolated from spleen using magnetic-assisted cell sorting (Miltenyi Biotec, Bergisch Gladbach, Germany) of CD115⁺ (streptavidin microbeads) or B220 (B220 beads). BMDMs were generated by culturing in RPMI1640 supplemented with 20% fibroblast-conditioned medium, which was generated by incubating log-phase L929 cells with RPMI1640 supplemented with 10% fetal calf serum. Fibroblasts secrete

macrophage colony-stimulating factor, which supports growth of macrophages from bone marrow stem cells. After 4 days of bone marrow cell culture, 50% of the medium of the serum was replaced with fresh fibroblast-conditioned medium. After 7 days of culture, BMDMs were harvested using a silicon-based cell scraper or were treated at day 6 for 24 hours with IL4 at a concentration of 20 ng/mL for alternative macrophage stimulation or with 100 ng/mL of interferon γ for 24 hours to generate classically activated macrophages. Two million cells were adoptively transferred into mice via intravenous injection.

Primary hepatocytes were isolated as described earlier in detail.²³ Primary HSCs were isolated from mouse livers, as described previously in detail.⁴⁵ HSCs in culture were stimulated with 100-ng/mL LPS, 25-ng/mL PDGF, or 1-ng/mL TGF- β (Peprotech, Hamburg, Germany).

Blood was taken from the right ventricle. Red blood cell lysis was done using Pharm Lyse (BD, Franklin Lakes, NJ) and was stopped using Hank's buffer salt solution supplemented with 5- μ M EDTA and 0.5% bovine serum albumin. Hepatic leukocytes were isolated from liver as described previously.⁴⁶ Single-cell suspensions were filtered using a 100- μ m mesh, and stained for flow cytometry, as described previously in detail.⁴⁶ Cells were isolated from liver by collagenase digestion, and erythrocytes were removed from Heparin-anticoagulated venous blood using PharmLyse lysing buffer (BD).

Cell Depletion by Antibodies and Clodronate Liposomes

The CD8-depleting antibody (clone TIB-210), the anti NK1.1⁺ cell-depleting antibody (clone PK-136), and the Gr1-depleting antibody RB6C were produced in the corresponding hybridoma cell lines (obtained from the American Type Culture Collection [Manassas, VA]). The antibodies were collected from the corresponding hybridomas and purified using fast protein liquid chromatography (detailed protocols are available upon request). Cell depletion was done using 250 depleting antibodies per mouse weighing 25 g. Commercial clodronate-loaded liposomes (Clodronate Liposomes, Haarlem, the Netherlands) were 2-fold concentrated using Vivaspin centrifugation concentrators (Sigma-Aldrich; Merck, Darmstadt, Germany) and a volume of 125 μ L as adapted for a mouse weighing 25 g was administered intravenously.

Analysis of mRNA Expression in Liver Tissue and Immune Cells

Liver pieces were snap-frozen in liquid nitrogen, and RNA was purified using the peqGold kit (PEQLAB Biotechnologie GmbH, Erlangen, Germany). RNA of sorted cells was isolated using the ArrayPure Nano-Scale RNA Purification Kit (Epicentre Biotechnologies, Madison, WI). Complementary DNA was generated from RNA using the First Strand complementary DNA synthesis kit (Roche, Penzberg, Germany). Quantitative real-time polymerase chain reaction was done based on SYBR Green reagent (Roche). Reactions

were done as triplicates, and β -actin was used to normalize gene expression.

Apoptosis Determination

The TUNEL assay performed on liver cryosections using the in situ cell death detection kit (Roche) according to manufacturer's instructions.

Statistical Analysis

All data are presented as mean \pm SD. Differences between groups were assessed by using the appropriate statistical tests (GraphPad Prism 5; GraphPad Software, San Diego, CA).

References

- Luedde T, Beraza N, Kotsikoris V, van Loo G, Nenci A, De Vos R, Roskams T, Trautwein C, Pasparakis M. Deletion of NEMO/IKK γ in liver parenchymal cells causes steatohepatitis and hepatocellular carcinoma. *Cancer Cell* 2007;11:119–132.
- Ringelhan M, Pfister D, O'Connor T, Pikarsky E, Heikenwalder M. The immunology of hepatocellular carcinoma. *Nat Immunol* 2018;19:222–232.
- Xue J, Schmidt SV, Sander J, Draffehn A, Krebs W, Quester I, De Nardo D, Gohel TD, Emde M, Schmidleithner L, Ganesan H, Nino-Castro A, Mallmann MR, Labzin L, Theis H, Kraut M, Beyer M, Latz E, Freeman TC, Ulas T, Schultze JL. Transcriptome-based network analysis reveals a spectrum model of human macrophage activation. *Immunity* 2014;40:274–288.
- Krenkel O, Puengel T, Govaere O, Abdallah AT, Mossanen JC, Kohlhepp M, Liepelt A, Lefebvre E, Luedde T, Hellerbrand C, Weiskirchen R, Longerich T, Costa IG, Anstee QM, Trautwein C, Tacke F. Therapeutic inhibition of inflammatory monocyte recruitment reduces steatohepatitis and liver fibrosis. *Hepatology* 2018;67:1270–1283.
- Krenkel O, Tacke F. Liver macrophages in tissue homeostasis and disease. *Nat Rev Immunol* 2017;17:306–321.
- Eggert T, Wolter K, Ji J, Ma C, Yevsa T, Klotz S, Medina-Echeverez J, Longerich T, Forgues M, Reisinger F, Heikenwalder M, Wang XW, Zender L, Greten TF. Distinct Functions of Senescence-Associated Immune Responses in Liver Tumor Surveillance and Tumor Progression. *Cancer Cell* 2016;30:533–547.
- Bartneck M, Schrammen PL, Mockel D, Govaere O, Liepelt A, Krenkel O, Ergen C, McCain MV, Eulberg D, Luedde T, Trautwein C, Kiessling F, Reeves H, Lammers T, Tacke F. The CCR2(+) Macrophage Subset Promotes Pathogenic Angiogenesis for Tumor Vascularization in Fibrotic Livers. *Cell Mol Gastroenterol Hepatol* 2019;7:371–390.
- Karlmark KR, Weiskirchen R, Zimmermann HW, Gassler N, Ginhoux F, Weber C, Merad M, Luedde T, Trautwein C, Tacke F. Hepatic recruitment of the inflammatory Gr1+ monocyte subset upon liver injury promotes hepatic fibrosis. *Hepatology* 2009;50:261–274.
- Mohs A, Kuttkat N, Reissing J, Zimmermann HW, Sonntag R, Proudfoot A, Youssef SA, de Bruin A, Cubero FJ, Trautwein C. Functional role of CCL5/RANTES for HCC progression during chronic liver disease. *J Hepatol* 2017;66:743–753.
- Tacke F. Cenicriviroc for the treatment of non-alcoholic steatohepatitis and liver fibrosis. *Expert Opin Investig Drugs* 2018;27:301–311.
- Schon HT, Bartneck M, Borkham-Kamphorst E, Nattermann J, Lammers T, Tacke F, Weiskirchen R. Pharmacological Intervention in Hepatic Stellate Cell Activation and Hepatic Fibrosis. *Front Pharmacol* 2016;7:33.
- Anstee QM, Neuschwander-Tetri BA, Wong VW, Abdelmalek MF, Younossi ZM, Yuan J, Pecoraro ML, Seyedkazemi S, Fischer L, Bedossa P, Goodman Z, Alkhouri N, Tacke F, Sanyal A. Cenicriviroc for the treatment of liver fibrosis in adults with nonalcoholic steatohepatitis: AURORA Phase 3 study design. *Contemp Clin Trials* 2019;89:105922.
- Lefebvre E, Moyle G, Reshef R, Richman LP, Thompson M, Hong F, Chou HL, Hashiguchi T, Plato C, Poulin D, Richards T, Yoneyama H, Jenkins H, Wolfgang G, Friedman SL. Antifibrotic Effects of the Dual CCR2/CCR5 Antagonist Cenicriviroc in Animal Models of Liver and Kidney Fibrosis. *PLoS One* 2016;11:e0158156.
- Kawano Y, Cohen DE. Mechanisms of hepatic triglyceride accumulation in non-alcoholic fatty liver disease. *J Gastroenterol* 2013;48:434–441.
- Liepelt A, Wehr A, Kohlhepp M, Mossanen JC, Kreggenwinkel K, Denecke B, Costa IG, Luedde T, Trautwein C, Tacke F. CXCR6 protects from inflammation and fibrosis in NEMO(LPC-KO) mice. *Biochim Biophys Acta Mol Basis Dis* 2019;1865:391–402.
- Zhang J, Zhao Y, Xu C, Hong Y, Lu H, Wu J, Chen Y. Association between serum free fatty acid levels and nonalcoholic fatty liver disease: a cross-sectional study. *Sci Rep* 2014;4:5832.
- Bitter A, Nussler AK, Thasler WE, Klein K, Zanger UM, Schwab M, Burk O. Human sterol regulatory element-binding protein 1a contributes significantly to hepatic lipogenic gene expression. *Cell Physiol Biochem* 2015;35:803–815.
- Knebel B, Hartwig S, Jacob S, Kettel U, Schiller M, Passlack W, Koellmer C, Lehr S, Muller-Wieland D, Kotzka J. Inactivation of SREBP-1a Phosphorylation Prevents Fatty Liver Disease in Mice: Identification of Related Signaling Pathways by Gene Expression Profiles in Liver and Proteomes of Peroxisomes. *Int J Mol Sci* 2018;19:980.
- Lefere S, Puengel T, Hundertmark J, Penners C, Frank AK, Guillot A, de Muyneck K, Heymann F, Adarbes V, Defrene E, Estivalet C, Geerts A, Devisscher L, Wettstein G, Tacke F. Differential effects of selective- and pan-PPAR agonists on experimental steatohepatitis and hepatic macrophages. *J Hepatol* 2020 Apr 29 [E-pub ahead of print].
- Wang Y, Nakajima T, Gonzalez FJ, Tanaka N. PPARs as Metabolic Regulators in the Liver: Lessons from Liver-Specific PPAR-Null Mice. *Int J Mol Sci* 2020;21:2061.

21. Candas D, Li JJ. MnSOD in oxidative stress response-potential regulation via mitochondrial protein influx. *Antioxid Redox Signal* 2014;20:1599–1617.
22. Marra F, Tacke F. Roles for chemokines in liver disease. *Gastroenterology* 2014;147:577–594.e1.
23. Bartneck M, Peters FM, Warzecha KT, Bienert M, van Bloois L, Trautwein C, Lammers T, Tacke F. Liposomal encapsulation of dexamethasone modulates cytotoxicity, inflammatory cytokine response, and migratory properties of primary human macrophages. *Nano-medicine* 2014;10:1209–1220.
24. Schwabe RF, Batailler R, Brenner DA. Human hepatic stellate cells express CCR5 and RANTES to induce proliferation and migration. *American journal of physiology Gastrointest Liver Physiol* 2003;285:G949–G958.
25. Mossanen JC, Tacke F. Role of lymphocytes in liver cancer. *Oncoimmunology* 2013;2:e26468.
26. Puengel T, Krenkel O, Kohlhepp M, Lefebvre E, Luedde T, Trautwein C, Tacke F. Differential impact of the dual CCR2/CCR5 inhibitor cenicriviroc on migration of monocyte and lymphocyte subsets in acute liver injury. *PLoS One* 2017;12:e0184694.
27. Bartneck M, Fech V, Ehling J, Govaere O, Warzecha KT, Hittatiya K, Vucur M, Gautheron J, Luedde T, Trautwein C, Lammers T, Roskams T, Jahnen-Dechent W, Tacke F. Histidine-rich glycoprotein promotes macrophage activation and inflammation in chronic liver disease. *Hepatology* 2016;63:1310–1324.
28. Starkey Lewis PJ, Moroni F, Forbes SJ. Macrophages as a Cell-Based Therapy for Liver Disease. *Semin Liver Dis* 2019;39:442–451.
29. Gschwandtner M, Derler R, Midwood KS. More Than Just Attractive: How CCL2 Influences Myeloid Cell Behavior Beyond Chemotaxis. *Front Immunol* 2019;10:2759.
30. Cao H, Chen X, Wang Z, Wang L, Xia Q, Zhang W. The role of MDM2–p53 axis dysfunction in the hepatocellular carcinoma transformation. *Cell Death Discovery* 2020;6:53.
31. Mitchell C, Couton D, Couty JP, Anson M, Crain AM, Bizet V, Renia L, Pol S, Mallet V, Gilgenkrantz H. Dual role of CCR2 in the constitution and the resolution of liver fibrosis in mice. *Am J Pathol* 2009;174:1766–1775.
32. Wood S, Jayaraman V, Huelsmann EJ, Bonish B, Burgad D, Sivaramakrishnan G, Qin S, DiPietro LA, Zloza A, Zhang C, Shafikhani SH. Pro-inflammatory chemokine CCL2 (MCP-1) promotes healing in diabetic wounds by restoring the macrophage response. *PLoS One* 2014;9:e91574.
33. Chu HX, Arumugam TV, Gelderblom M, Magnus T, Drummond GR, Sobey CG. Role of CCR2 in inflammatory conditions of the central nervous system. *J Cereb Blood Flow Metab* 2014;34:1425–1429.
34. Lucas T, Waisman A, Ranjan R, Roes J, Krieg T, Muller W, Roers A, Eming SA. Differential roles of macrophages in diverse phases of skin repair. *J Immunol* 2010;184:3964–3977.
35. Skat-Rørdam J, Højland Ipsen D, Lykkesfeldt J, Tveden-Nyborg P. A role of peroxisome proliferator-activated receptor γ in non-alcoholic fatty liver disease. *Basic Clin Pharmacol Toxicol* 2019;124:528–537.
36. Li X, Yao W, Yuan Y, Chen P, Li B, Li J, Chu R, Song H, Xie D, Jiang X, Wang H. Targeting of tumour-infiltrating macrophages via CCL2/CCR2 signalling as a therapeutic strategy against hepatocellular carcinoma. *Gut* 2017;66:157–167.
37. Teng KY, Han J, Zhang X, Hsu SH, He S, Wani NA, Barajas JM, Snyder LA, Frankel WL, Caligiuri MA, Jacob ST, Yu J, Ghoshal K. Blocking the CCL2-CCR2 Axis Using CCL2-Neutralizing Antibody Is an Effective Therapy for Hepatocellular Cancer in a Mouse Model. *Mol Cancer Ther* 2017;16:312–322.
38. Liang YJ, Luo J, Lu Q, Zhou Y, Wu HW, Zheng D, Ren YY, Sun KY, Wang Y, Zhang ZS. Gene profile of chemokines on hepatic stellate cells of schistosomosome-infected mice and antifibrotic roles of CXCL9/10 on liver non-parenchymal cells. *PLoS One* 2012;7:e42490.
39. Halama N, Zoernig I, Berthel A, Kahlert C, Klupp F, Suarez-Carmona M, Suetterlin T, Brand K, Krauss J, Lasitschka F, Lerchl T, Luckner-Minden C, Ulrich A, Koch M, Weitz J, Schneider M, Buechler MW, Zitvogel L, Herrmann T, Benner A, Kunz C, Luecke S, Springfield C, Grabe N, Falk CS, Jaeger D. Tumoral Immune Cell Exploitation in Colorectal Cancer Metastases Can Be Targeted Effectively by Anti-CCR5 Therapy in Cancer Patients. *Cancer Cell* 2016;29:587–601.
40. Ochoa-Callejero L, Perez-Martinez L, Rubio-Mediavilla S, Oteo JA, Martinez A, Blanco JR. Maraviroc, a CCR5 antagonist, prevents development of hepatocellular carcinoma in a mouse model. *PLoS One* 2013;8:e53992.
41. Moroni F, Dwyer BJ, Graham C, Pass C, Bailey L, Ritchie L, Mitchell D, Glover A, Laurie A, Doig S, Hargreaves E, Fraser AR, Turner ML, Campbell JDM, McGowan NWA, Barry J, Moore JK, Hayes PC, Leeming DJ, Nielsen MJ, Musa K, Fallowfield JA, Forbes SJ. Safety profile of autologous macrophage therapy for liver cirrhosis. *Nat Med* 2019;25:1560–1565.
42. Thomas JA, Pope C, Wojtacha D, Robson AJ, Gordon-Walker TT, Hartland S, Ramachandran P, Van Deemter M, Hume DA, Iredale JP, Forbes SJ. Macrophage therapy for murine liver fibrosis recruits host effector cells improving fibrosis, regeneration, and function. *Hepatology* 2011;53:2003–2015.
43. Kellendonk C, Opherck C, Anlag K, Schutz G, Tronche F. Hepatocyte-specific expression of Cre recombinase. *Genesis* 2000;26:151–153.
44. Wehr A, Baeck C, Ulmer F, Gassler N, Hittatiya K, Luedde T, Neumann UP, Trautwein C, Tacke F. Pharmacological inhibition of the chemokine CXCL16 diminishes liver macrophage infiltration and steatohepatitis in chronic hepatic injury. *PLoS One* 2014;9:e112327.
45. Bartneck M, Warzecha KT, Tag CG, Sauer-Lehnen S, Heymann F, Trautwein C, Weiskirchen R, Tacke F. Isolation and time lapse microscopy of highly pure hepatic stellate cells. *Anal Cell Pathol* 2015;2015:417023.

46. Bartneck M, Ritz T, Keul HA, Wambach M, Bornemann J, Gbureck U, Ehling J, Lammers T, Heymann F, Gassler N, Ludde T, Trautwein C, Groll J, Tacke F. Peptide-functionalized gold nanorods increase liver injury in hepatitis. *ACS Nano* 2012;6:8767–8777.

Reprint requests

Address requests for reprints to: Frank Tacke, MD, PhD, Department of Hepatology & Gastroenterology, Charité Universitätsmedizin Berlin, Augustenburger Platz 1, 13353 Berlin, Germany. e-mail: frank.tacke@charite.de; fax: +49-30-450-553902.

Acknowledgments

The authors cordially thank Michelle Frohn, Aline Roggenkamp, and Carmen Tag for assistance with the experiments.

CRedit Authorship Contributions

Matthias Bartneck (Conceptualization: Lead; Data curation: Lead; Formal analysis: Lead; Methodology: Lead; Supervision: Lead; Writing – original draft: Lead; Writing – review & editing: Lead)

Christiane Koppe (Conceptualization: Supporting; Methodology: Equal; Resources: Equal)

Viktor Fech (Data curation: Equal; Methodology: Equal)

Klaudia T Warzecha (Formal analysis: Supporting; Investigation: Supporting; Methodology: Supporting)

Marlene Kohlhepp (Formal analysis: Supporting; Investigation: Supporting)

Sebastian Huss (Validation: Supporting; Visualization: Equal)

Ralf Weiskirchen (Investigation: Supporting)

Christian Trautwein (Project administration: Supporting)

Tom Luedde (Conceptualization: Equal)

Frank Tacke (Conceptualization: Lead; Funding acquisition: Lead; Methodology: Equal; Project administration: Lead; Writing – original draft: Equal; Writing – review & editing: Equal).

Conflicts of interest

The authors disclose no conflicts.

Funding

This work was supported by the German Research Foundation (DFG Ta434/3-1 to Frank Tacke, BA 6226/2-1 to Matthias Bartneck, CRC 1382 to Frank Tacke, CRC/TRR 57 to Frank Tacke, CTC/TRR 296 to Frank Tacke), the Wilhelm Sander Foundation (Grant no. 2018.129.1 to Matthias Bartneck), and the EFRE.NRW initiative (I3-STM to Frank Tacke).